

THE EFFECT OF HYDROGEN PLASMA TREATMENT ON DAMAGED AND
AND UNDAMAGED MIS SOLAR CELLS

by

Laila Saleh Babsail

B.Sc., Cairo American University, Egypt, 1982.

THESIS SUBMITTED IN THE PARTIAL FULFILLMENT OF THE
REQUIREMENTS FOR THE DEGREE OF MASTER OF SCIENCE
in the Department
of
Physics



Laila Saleh Babsail

SIMON FRASER UNIVERSITY

November, 1988.

All rights reserved. This work may not be reproduced in whole or in part, by photocopy or other means, without permission of the author.

Approval

Name: Laila Saleh Babsail

Degree: Master of Science

Title of Thesis: The effect of hydrogen plasma treatment on
damaged and undamaged MIS solar cells.

Examining Committee:

Chairperson: E. D. Crozier

S.R. Morrison
Senior Supervisor

R.F. Frindt

M.L.W. Thewalt

K. Colbow
External Examiner

Date Approved: November 16, 1988

PARTIAL COPYRIGHT LICENSE

I hereby grant to Simon Fraser University the right to lend my thesis, project or extended essay (the title of which is shown below) to users of the Simon Fraser University Library, and to make partial or single copies only for such users or in response to a request from the library of any other university, or other educational institution, on its own behalf or for one of its users. I further agree that permission for multiple copying of this work for scholarly purposes may be granted by me or the Dean of Graduate Studies. It is understood that copying or publication of this work for financial gain shall not be allowed without my written permission.

Title of Thesis/Project/Extended Essay

The Effect of Hydrogen Plasma Treatment on Damaged and
Undamaged MIS Solar Cells.

Author:

(signature)

Laila Saleh Babsail

(name)

Dec. 12, 1988

(date)

Abstract

A metal-insulator-semiconductor structure was used to study the effect of hydrogen plasma treatment on solar cells. Hydrogen plasma treatment is found to improve the performance of poly-crystalline, amorphous silicon cells and leads to the improvement of the Si-SiO₂ interface.

Cells were fabricated on crystalline silicon and are treated in hydrogen plasma for different exposure times. This has led to changes in I-V characteristics and a noticeable drop in the photocurrent and density of charge carriers with exposure time. This in turn leads to a drop in the solar cell efficiency. The open circuit voltage drops only after longer periods of exposure times.

Other cells were fabricated on damaged silicon, the damage created by lapping the silicon surface. The silicon was then exposed to hydrogen plasma after the system had been evacuated, leading to an over all improvement in the performance of the solar cell.

The effect of heating silicon in molecular hydrogen has created some controversy in the literature and it was not clear if it had positive effect on the damaged samples. This experiment shows that heating damaged samples in molecular hydrogen reduces the dark reverse saturation current.

Heating the samples in the process of fabrication to temperatures higher than 500 °C does not drive the hydrogen completely out of the samples. Measurements taken up to 8

months after fabrication still detect the effects of hydrogen.

It is concluded that hydrogen plasma exposure has beneficial and degrading effects. It improves solar cell characteristics when they have been degraded by dislocations, but it deactivates acceptors in the p-silicon leading to poorer characteristics. Further studies are needed to attain the best compromise and to optimize the cells made from low quality silicon.

Acknowledgement

I would like to thank Dr. Morrison for his patience during the discussions we had that made the physics clear. I am also grateful for Ranjith Divigalpitya for plenty of help during the experiment and while writing up, and for helping me understand his model. I would like to thank Jae-Gwang Lee for allowing me to make use of his figures and Kanthi Kaluarachchi for her support and proof reading the thesis.

I wish to thank my supervisory committee especially Dr. Frindt for helping me out while Dr. Morrison was away. I am also grateful to my sponsors, King Saud University.

Lastly, I would like to acknowledge people in my lab and outside who I had discussions with and helped me understand more about my thesis and other matters.

Chapter II Experiment and Measurement	16
2.1 Sample preparation	16
2.1.1 Cleaning the Silicon	16
2.1.2 Back Contact	16
2.1.3 Oxide	16
2.1.4 Front Contact	17
2.1.5 Damaged samples	17
2.1.6 Passivation	18
2.2 Measurements and Instrumentation	20
2.2.1 The equipment	20
2.2.2 Sample measurement	
2.2.3 Interpretation of Capacity measurement	22
Chapter III Experimental results	30
3.1 Undamaged substrate	30
3.1.1 The effect of a H plasma on solar cell parameters	31
3.1.2 Stability of the characteristics after plasma treatment	32
3.1.3 The effect of molecular Hydrogen	33
3.2 The solar cell with surface dislocation	33
3.2.1 Effect of the hydrogen plasma	34
3.2.2 Effect of molecular hydrogen	35
3.2.3 Stability of passivation of molecular and hydrogen plasma treatments	36
Chapter IV Discussion and Conclusion	47
4.1.1 Undamaged samples	47

4.1.2 Damaged samples	50
4.2 Conclusions	52
Bibliography	58

LIST OF TABLES

Table I	Undamaged samples	37
TableII	Damaged samples	38

LIST OF FIGURES

1-1	The current voltage characteristics of the solar cell	12
1-2	Dislocation line	13
1-3	The effect of SCR due to dislocation on the energy band diagram	14
1-4	The band diagram according to the model	15
2-1	The MIS solar cell structure	25
2-2a	Schematic diagram of the vacuum evaporator	26
2-2b	The rotatable mask holder	26
2-3	The hydrogen passivation apparatus	27
2-4	Measuring device for the solar cell characteristics	28
2-5	The electrical circuit used in measuring I/V and C/V	29
3-1	The variation of V_{oc} with passivation time	39
3-2	The variation of I_{sc} with passivation time	40
3-3	The variation of FF with passivation time	41
3-4	The variation of Efficiency with passivation time	42
3-5	The variation of Charge carriers with passivation time	43
3-6	The I-V characteristics of solar cells in the dark and under illumination	44
3-7	Damaged samples I-V characteristics under illumination	45
3-8	Damaged samples I-V characteristics in the dark	46
4-1	The variation of $1/C^2$ with the voltage for undamaged samples and no hydrogen treatment	55

4-2	The variation of $1/C^2$ with the voltage for undamaged samples with $3\frac{1}{2}$ hours hydrogen plasma treatment	56
4-3	The variation of the current density with the voltage from the model for different energies	57

Chapter I

1.Introduction:

This is to report a study of the influence of surface damage on the efficiency of MIS (metal insulator semiconductor) silicon solar cells, and of the influence of hydrogen introduced to passivate the damage. MIS silicon cells represent an important approach to the development of low cost solar cells, but to realize their potential, low cost silicon must be used, where many defects are present. In this study we modeled the defects by introducing lapping damage to the silicon surface, and then studied the passivation of the damage.

As will be described in the thesis, the influence of the hydrogen is complex, because with the p-silicon used in the MIS cells, the hydrogen does not only interact with impurities but also with the acceptors in the silicon. Thus it was necessary to study both undamaged and damaged silicon in order to separate the two interactions.

1.1.Metal insulator semiconductor:

The ideal MIS solar cell operates like an n^+p junction ^{1,2,3} since for optimum design the surface of the semiconductor should be inverted over the range of bias voltage usually encountered. The fermi energy should thus be (and is reported in the literature to be) close to the conduction band edge at the interface. The dark current is then controlled by processes within the semiconductor and consists of injection-diffusion and

recombination components¹. The diffusion current is given by³

$$J_{diff} = J_{od} [\exp(qV_j/kT) - 1] \quad (1.1)$$

where J_{od} is the saturation injection diffusion current density. V_j the voltage across the junction. T , k and q have their standard meaning. The recombination current can be written

$$J_{rec} = (qn_i W / \tau_e) \exp(qV_j/2kT) \quad (1.2)$$

for values of V_j greater than a few kT/q . W is the width of the semiconductor depletion region, n_i the density of charge carriers in an intrinsic semiconductor, and τ_e is the effective lifetime of the charge carriers. Fig.1-1 shows the I-V behaviour of these cells under illumination. The fill factor

$$FF = V_m J_m / V_{oc} J_{sc} \quad (1.3)$$

where J_m and V_m are the current density and voltage at the maximum power point (viz where $I.V$ is maximum), J_{sc} and V_{oc} are the short circuit current and the open circuit voltage respectively. The efficiency of the cell is defined as:

$$\text{Efficiency} = FF J_{sc} V_{oc} / P_{input} \quad (1.4)$$

where P_{input} is the power density of illumination on the solar cell.

1.2.Introducing hydrogen to silicon:

It is possible to introduce hydrogen in the near surface region of Si, by various techniques by exposure to hydrogen plasma, avalanche injection or by polishing in a slurry of Al_2O_3 powder and water ^{4,5}. It has been found that Schottky diodes made from boron doped p-type Si showed significant deactivation of their shallow acceptor density when boiled in water as determined by measurements of changes in the near surface bulk resistivity ⁶. It has also been found that all shallow acceptors in Si (eg. B, Al, Ga, In and Tl) are passivated by reaction with atomic hydrogen at temperatures above 100 °C ⁷. However, there is some conflict about the maximum temperature at which the passivation is still stable and whether or not molecular hydrogen has any effect on the solar cells. Sections 1.2.1 and 1.2.2 present related studies from the literature on crystalline and polycrystalline solar cells.

1.2.1.Effect of Hydrogen in single crystal, undamaged silicon:

1.2.1.1.Passivation of various defects:

The observation that atomic hydrogen, introduced as described above, passivates shallow and deep impurities in crystalline Si (c-Si) has led to intense interest in this area. Hydrogen passivation of shallow dopants, as opposed to compensation, is generally accompanied by distinctive changes in the transport properties of a doped sample. The carrier

concentration of samples is observed to decrease while the Hall mobility increase^{8,9}. Atomic hydrogen (H) is able to migrate in c-Si at low temperature (≤ 400 °C) and to bond to both shallow and deep level impurities, passivating their electrical activity¹⁰. Hydrogen passivates unreconstructed surface dangling bonds and trivalent Si defects at the Si-SiO₂ interface^{7,11}. Low temperature SIMS and IR spectroscopy experiments have shown that the bonding was primarily between Si and H and the depth of H passivation in c-Si is few μm . Typically passivation has been done at temperatures around 100-200 °C, exposing the silicon to either a plasma created by a Kaufman ion source⁷ for a few minutes or a plasma created by rf discharge for a few hours^{12,13}. In a study conducted by Sah et al.¹⁴ it was concluded that interstitial atomic H is very reactive and mobile. According to Johnson et al.¹⁵ passivation of the bulk acceptor impurities is by insertion of H atoms between substitutional acceptor and an adjacent Si atom so as to form a Si-H and a neutralized threefold coordinated acceptor.

It is obvious that hydrogen interacts with impurities and other defects in the crystalline silicon.

1.2.1.2. Stability of passivation under heat treatment:

In a review paper by Pearton et al.⁷ they claim that hydrogen passivation of deep levels is thermally unstable at temperatures above 400 °C. The neutralized boron acceptors in silicon are almost completely re-activated after a 5 minutes anneal at temperature around 200 °C⁷. Upon annealing to restore

the acceptor activity, however, SIMS measurements show ⁷ that the hydrogen has not moved on a macroscopic scale; it is still in the silicon. The new form of hydrogen is not removed from the Si until heating at approximately 600 °C, many hundreds of degrees above the temperature required to reactivate the acceptors. At the concentration at which it is present, this stable form of hydrogen cannot be bonded to defects or other impurities and the logical conclusion is that it is molecular hydrogen⁷. Thewalt et al.¹⁶ used photoluminescence spectroscopy to verify that low temperature treatment in a hydrogen plasma can neutralize the B, In and Tl acceptors in Si and they found that all the neutral complexes are unstable when heated at 300 °C under vacuum. Stutzmann¹⁷ has shown that passivation is completely reversible if annealed at 200 °C for 30 minutes.

1.2.1.3.Molecular Hydrogen:

Molecular hydrogen (H₂) from the gas phase causes no changes in silicon. If any H₂ is introduced, it is electrically and optically inactive and essentially immobile at low temperature (<500 °C)⁷. Point defects in crystalline silicon are neutralized by hydrogen plasma but not by molecular hydrogen¹¹.

1.2.2.Damaged Samples:

1.2.2.1.Effect of Hydrogen on polycrystalline or damaged Si:

Hydrogen plasma treatment has led to improvement in the performance of solar cells with grain boundaries (GB's) and

intergrain defects. It reduces their influence, viz the trapping states associated with these defects are made electrically inactive¹⁸. It is well established that GB's can offer substantial impedance to majority carrier current flow in Si. Solar cell performance studies have shown that GB's also act as strong recombination centers¹⁹. On passivation of upgraded metallurgical grade Si poly-crystalline cells, the solar cell characteristics showed marked increases in V_{oc} , FF and efficiency. The increase was greater when the initial values were smaller. Specifically, atomic H is believed to result in a reduction of barrier heights, electrical resistance and recombination⁵. Seager et al.²⁰ concludes that the improvement is from removal of GB's trapping states. Ammor et al.²¹ found that the interfacial recombination velocity at GB's decreases causing the effective diffusion length to increase after hydrogenation. Interfacial recombination velocity at most GB's is reduced about 10 to 20 times and dislocation recombination disappears when the EBIC images are contrasted^{20,22}. H plasma passivation has also been shown to reduce the diode reverse leakage current⁵.

1.2.2.2. Hydrogen diffusion in Grain Boundaries:

Published data on the diffusion of atomic hydrogen in Si, indicates that the diffusion constant in the bulk is smaller than that in the grain boundaries by a factor of at least several orders of magnitude (10^6)^{23,24}. It is obvious that hydrogen leads to improvement in the performance of solar cell

made of polycrystalline Si by reducing the barrier height and also the minority carrier recombination in the grain boundaries. No significant increase in J_{sc} is observed since the grains are large and recombination at GB's would account for a loss in J_{sc} of only about 2%.⁵ Note that the short circuit current density following passivation tends to a limiting value approximately 23 mA/cm² at AM1 conditions. The beneficial effect of passivation seems to be particularly manifested in V_{oc} .²⁵

1.2.2.3. Effect of Heat treatments on Passivated Defects:

If hydrogen implanted polycrystalline Si wafers are annealed at 450 °C in Ar for 30 minutes and then subsequently metallized to make Schottky diodes, the I-V characteristics are again found to display barrier enhancement, a higher barrier at the GB's and rectification²⁶. Overstraeten¹⁸ stated that hydrogen is easier to remove than claimed by Mu et al.²⁶; if samples are heated above 400 °C the hydrogen escapes completely from the sample. The outgassing rate of H from hydrogenated a-Si (amorphous Si) films has been shown to be maximum at around 375 °C¹⁹. Other papers (refs 27, 21, 28) quote H as more stable in polycrystalline silicon. At 400 °C the diffusion process can proceed in either direction, either deeper into the sample, or out through the surface. At a temperature of 450 °C the out diffusion becomes more pronounced than at 400 °C²⁷. Ammor et al.²¹ found H in GB has binding energy between 1.5 and 3.4 eV, thus a temperature higher than 400 °C is required for H to leave the polycrystal. Nuclear reaction analysis performed after 400

°C thermal anneal showed that the out-diffusion H content is small (about 20% of the original)²⁸. Lastly Rao et al.²⁹ found that the positive effect of a 10 hour hydrogen plasma treatment is retained, even after heating the samples to 580 °C for a few minutes.

Experiments done on hydrogen stability does not agree on the temperature at which hydrogen starts to out diffuse. Some find hydrogen to be stable to 400 °C others to 450 °C another claim the hydrogen is in the Si even after heating the sample to 580 °C.

1.2.2.4.Molecular Hydrogen:

It is generally accepted that treatment using molecular H does not influence the properties of bulk defects in Si¹⁸. For example Meier et al. found that an exposure to molecular H at 300 °C for 4 hours was ineffective in neutralizing point defects³⁰. Because molecular H is ineffective, passivation is commonly achieved either by molecular H dissociation in a glow discharge or by low energy atomic H implant by an ion gun.⁴ However Sardi et al. (ref 31) claim to have established that both atomic and molecular H diffusion considerably enhance the efficiency of semicrystalline solar cells. They found the spreading resistance in semicrystalline Si before H₂ diffusion to be 2.6 ohm cm and after H₂ diffusion to be 1.59 ohm cm (t=500 °C for 1 hour).

1.3.Dislocations:

In next two sections the dislocation is defined and a model is reviewed that describes its effect on solar cells.

1.3.1.The Dislocation:

Application of a stress, for example plastic deformation, on the crystal may rupture some of the Si-Si bonds^{32,33}. When these bonds are broken Si atoms are left with an unpaired electron and these are referred to as dangling bonds. A line dislocation has an array of dangling bonds, Fig. 1-2 (ref.33), that will act as traps. Glaenzer et al.³⁵ found that in p-type silicon the dislocation is found to have a donor level, in other words it is a positively charged line with a cylindrical negative space charge region around it. Fig.1-3 after ref.34 shows a dislocation in p-type material leading to the formation of a trap level in the energy band.

1.3.2.Dislocation Model:

A model was proposed by Divigalpitiya and Morrison ³³, for MIS solar cells with surface dislocation loops describing how these dislocation loops at the surface (produced by mechanically polishing the surface as was done in the present work) degrade the solar cell characteristics. Their model will be reviewed briefly to show how lowering the potential barrier affects the I-V characteristics.

The depth of the damaged region, where dislocations form, has been shown to be comparable to the size of the particles used for lapping to create the dislocations. This means the

dislocations created by particles of size $1\mu\text{m}$ would extend beyond the space charge region (SCR) at normal range of bias voltage (-1 to 1 v). For theoretical modelling, the dislocation loops are considered to be of uniform distribution, dislocation lines running perpendicular to the surface of Si. It is known that dislocations in p-type material have donor levels in the band gap ³⁶, these will be referred to as E_t . Close to the surface, E_t is assumed to be aligned with the metal fermi level since the electrons can easily tunnel through the thin oxide. In the model, it was assumed that the dislocations have a certain conductivity for carriers in these levels that allows the carriers to move along the potential gradient which is established by the carrier movement itself. Then ohm's law applies:

$$I_d(x) = -s dV_d(x)/dx \quad (1.5)$$

where I_d is the electron current along the defect levels, s is the specific conductance, V_d is the difference between the the trap energy and the metal fermi energy divided by q , where q is the charge of electron (fig. 1-4). A second equation used is that of continuity of carriers

$$d[I_d(x)]/dx = -qK_p p_d \quad (1.6)$$

where K_p is the rate constant for hole capture at the dislocation and p_d is the density of holes at the dislocation.

Fig.1-4 shows the energy band diagram of a p-type MIS solar cell with surface dislocations. For a more detailed discussion of the applicability and meaning of this model, see ref.33.

The above two equations are to be solved with two boundary conditions. The first boundary condition arises because most of the electrons are generated beyond the damaged region (L_n is approximately $100 \mu\text{m}$ while the damaged region only extends approximately $1\mu\text{m}$). Thus the minority carrier current captured by the dislocations is assumed independent of the applied voltage for a given light intensity and dislocation density, it is a constant of the system. For simplicity of analysis it is assumed this minority carrier current is captured at the end of the dislocation, so that the minority carrier current at $x=l$ is constant. A second boundary condition assumes that the density of trap levels at the dislocation is high enough that carrier exchange with the metal makes the trapping level at the surface isoenergetic with the metal fermi energy. The solution becomes

$$I_{dl} = \pm s [B \exp(\beta V_o) + C]^{1/2} \quad (1.7)$$

C is the integration constant, V_o is the output voltage (bias voltage), and

$$B = [qK_p p_d \exp-(E_1 - \mu) / kT] / s \quad (1.8)$$

$$E_1 = q(V + V_o + V_d) + \mu \quad (1.9)$$

where V is $(E_v - E_{v,d})/q$ and μ is the difference between the semiconductor fermi level E_{fs} and the valence band energy E_v .

Discussion will be continued in section 4.1.2 to show how change in $(E_v - \mu)$ affect the I-V behaviour of the solar cell.

$$J = I_{dl} D_{dl} + \alpha J_b \quad (1.10)$$

The above is the expression for the total current density, where D_{dl} is the number of dislocations, α is a geometrical factor and J_b is the undamaged current density.

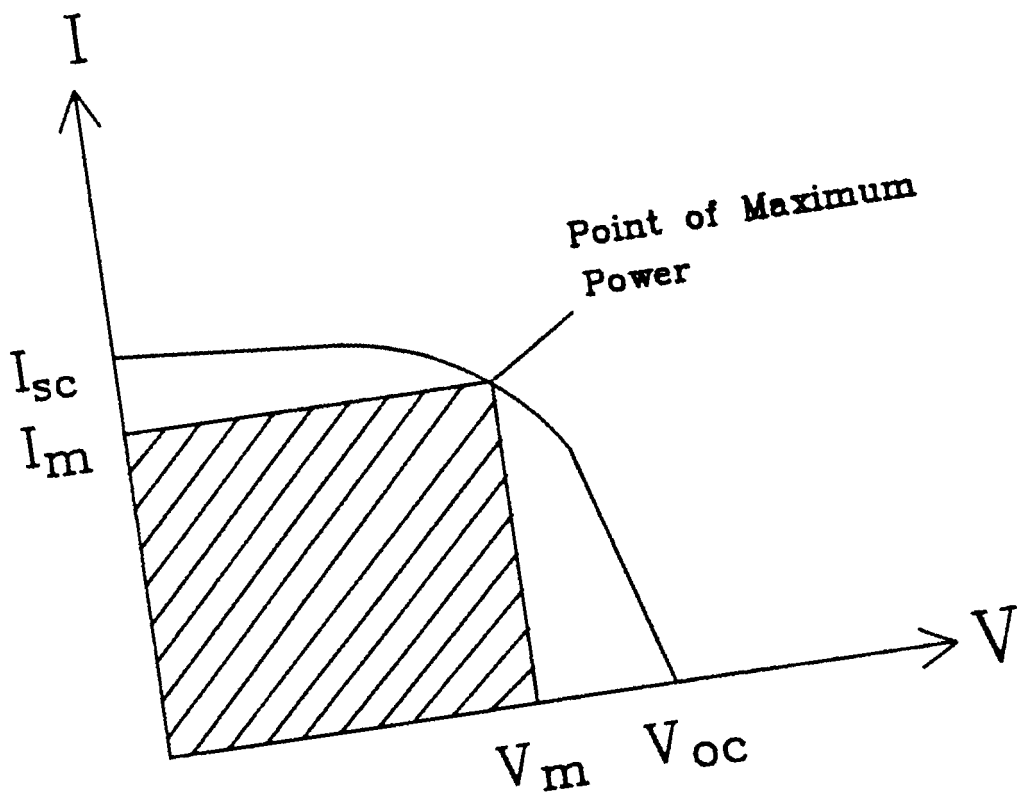


Fig. 1-1 The current voltage characteristics of the solar cell

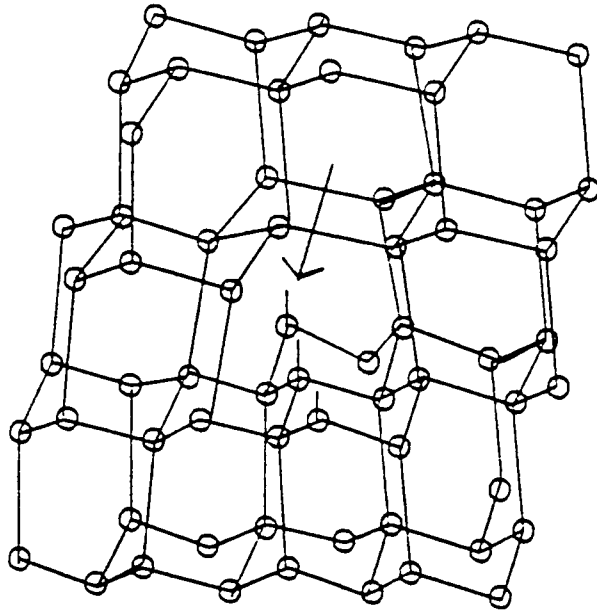


Fig 1-2 Dislocation line. The arrow pointing at one of the dangling bonds in the dislocation line.

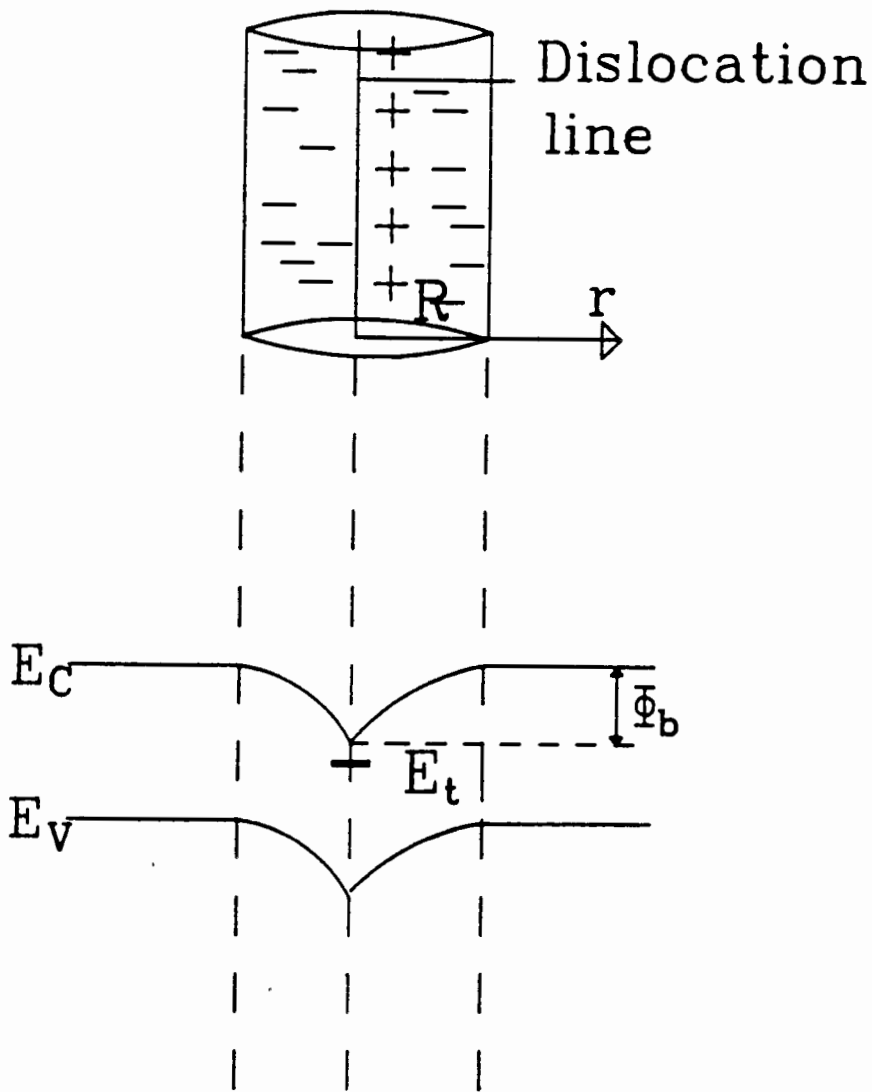


Fig 1-3 The effect of the SCR due to dislocation on the energy band diagram

R is the radius of the space charge region.

Φ_b is the potential barrier.

E_t is a trap level in the energy band due to dislocations

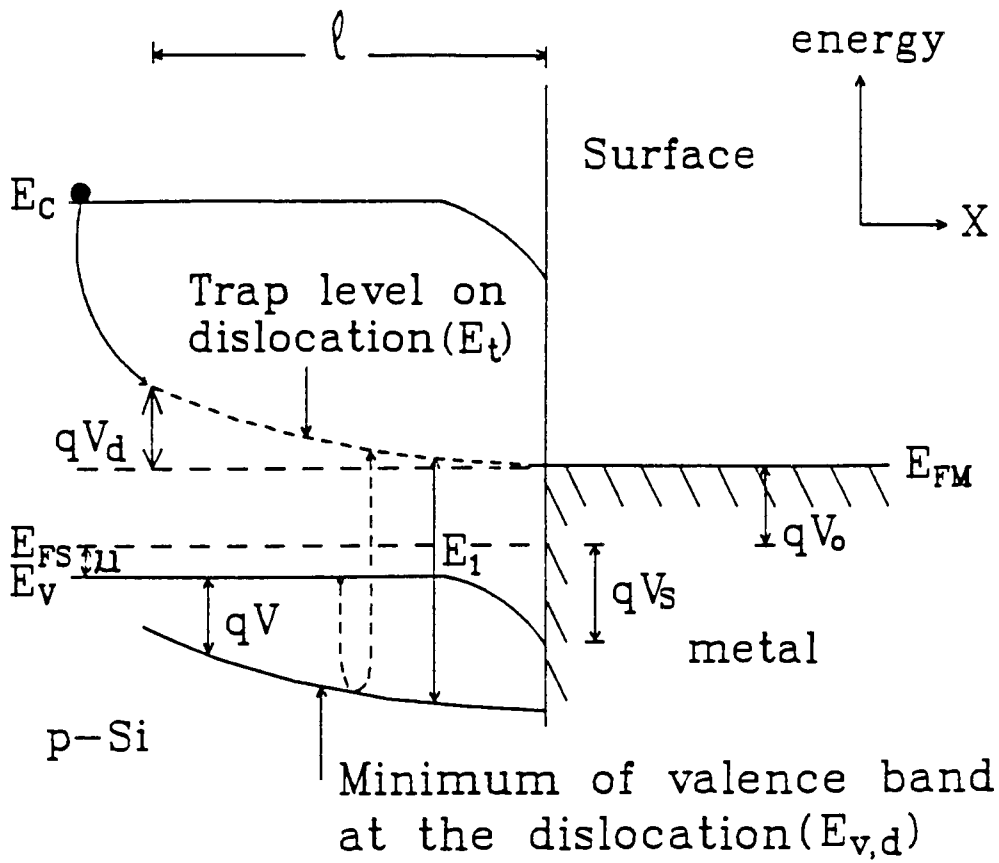


Fig 1-4 The band diagram according to the model (Ref.33).

Chapter II

2. Experiment and Measurement:

2.1. Sample preparation:

2.1.1. Cleaning the Silicon:

Solar cells were made with p-type (boron doped) Si single crystal wafers, of <100> orientation, thickness 475-575 μm , and resistivity ranging from 5-8 ohm cm, cut into 1 cm^2 squares. Care was used in handling the samples to avoid introducing surface dislocations. The samples were degreased by sequential rinses in trichloroethylene, acetone, methanol and deionized water. Then they were etched in 10% hydrofluoric acid for a minute to remove the native oxide, rinsed again with deionized water and dried under blowing nitrogen gas.

2.1.2. Back contact:

Directly after being cleaned, the samples were placed in the vacuum evaporator where an Al contact of 1500 Å thickness was deposited on the back of the Si.

2.1.3. Oxide:

The front surface of the wafer was oxidized and the back contact annealed for good ohmic contact in the same step. The samples were introduced into a quartz tube, and placed inside a Lindberg furnace at a temperature of 520 °C. Argon was allowed

to flow for the first 5 minutes, followed by high purity O₂ (minimum purity 99.6%) for another 5 minutes to form the insulating layer of silicon oxide on the surface, and finally the gas was switched back for another 5 minutes of Ar flow. The furnace was then switched off and the samples were left in Ar flow at one end of the tube to cool and anneal for approximately 40 minutes. The thickness of the grown oxide layer, measured by an ellipsometer, was found to be $18 \pm 3 \text{ \AA}^{33}$.

2.1.4. Front contact:

The samples were placed again in the vacuum evaporator to deposit a thin circular layer of high purity (99.99% pure) Al, of 50 Å thickness thin enough that during the measurement of solar parameters it would not block the light significantly. Then, with the aid of rotating mask, a finger pattern of 200 Å thick Al was also deposited to ensure good contact to the 50 Å layer. The front contact had an effective area of 0.37 cm². Fig.2-1 shows the structure of the completed MIS cell.

2.1.5. Damaged samples:

If samples were to be damaged by lapping, this was done after the the back contact was deposited (section 1.1.2). Dislocations were introduced to the surface by lapping in a slurry of Al₂O₃. The dislocations so produced are in the form of loops since a dislocation normally starts and ends at a surface³⁷.

For lapping, water was added to polishing powder (Al₂O₃

obtained from BaikaloX Cooperation, California, particle size 1 micron). This slurry was kept in an ultrasonic bath for 5 minutes to disperse any agglomerates. About 2 ml of the agglomerate free slurry was transferred on to a clean glass plate where the front side of Si was hand lapped for 1 minute. Samples were then washed by deionized water and ultrasonicated for a few minutes to ensure there were no alumina particles adhering to the surface.

2.1.6. Passivation:

To study the effect of hydrogen some samples were subjected to molecular H and others to hydrogen plasma treatment. The passivation treatment was done after the back contact deposition and before oxidation. Following ref.19, H radicals were produced by high frequency alternating fields of a tesla coil. The apparatus is sketched in Fig 2-3. The tube was evacuated and flushed with ultra high purity (U.H.P. Linde) hydrogen (minimum purity 99.9999%). This was repeated twice to minimize contaminants in the system. The tube was then back filled with H₂ from pressures of 10⁻⁵ torr or 10⁻⁶ torr to approximately 20 mtorr which gave a homogeneous plasma when the tesla coil was switched on. The samples were heated to a high temperature (approximately 380 °C) for 3 hours. The fraction of time that the plasma was turned on was variable. After the 3 hours the samples were left to cool for ½ hour. In the case of the 3½ hours plasma treatment the plasma was still on while the samples were cooling.

Undamaged samples were passivated for different periods of time to study the effect of hydrogen on the solar cell characteristics. The exposure of undamaged samples to the H plasma was for periods of 5, 10, 20, 40, 80 minutes, and 3½ hours. Some samples were heated in molecular H₂. Samples were then removed to form the oxide.

The damaged samples were all treated at 380 °C for 3½ hour in either plasma or molecular H₂. In the last ½ hour the heater was switched off and the samples were either left to cool in H plasma or molecular hydrogen.

All samples were etched in 10% HF (hydrofluoric acid) for 30 seconds before the oxidation step was carried out. Lastly they were transferred to the evaporator for the front contact. Only one sample is passivated at a time and the process requires from 7-8 hours to make a solar cell.

Whenever a sample was passivated an unpassivated "blank" was prepared, then both went through the same treatment for comparison.

It is worth noting that adding oxygen to a hydrogen plasma does increase the yield of monatomic hydrogen³⁸. The plasma is a conglomerations of positive and negative ions, molecules, neutral atoms and free radicals, which is neutral overall. Addition of small amounts of H₂O or O₂ (0.1-0.3%) can reduce recombination in H plasma, and increase the production of H ions by more than an order of magnitude⁷. It is presumed that samples done after the system was evacuated to a pressure of 10⁻⁵ torr have a higher oxygen partial pressure than when the

system was evacuated to 10^{-6} torr.

2.2. Measurements and Instrumentation:

2.2.1. The equipment:

The vacuum evaporator with an oil diffusion pump and a liquid nitrogen baffle, provided a minimum pressure of 10^{-7} torr. The evaporator was equipped with a quartz crystal thickness monitor which can be used to measure the thickness of deposited film to an accuracy of ± 1 Å. Al pellets were placed in tungsten boats, where high currents could be passed to melt the pellets. To deposit the front contact, the circular layer of 50 Å and the finger pattern of 200 Å, a mask was used. Fig. 2-2 shows the apparatus schematically.

The passivation system consisted of a quartz tube, connected to a vacuum pump, with a cylindrical furnace around it allowing one to heat the sample during passivation. To measure the temperature a thermocouple was placed between the outside wall of the tube and the heater. Fig 2-3 shows the apparatus.

The samples were mounted on a sample holder which was placed in a light tight housing. The housing had a shutter to allow illumination of the sample. The source of illumination was a 150 W Xe arc lamp adjusted with Oriel filter to simulate the solar sun. The standard intensity used was 100 mW/cm^2 . Fig.2-4 shows a schematic diagram of the measuring equipment of the solar cell.

2.2.2. Sample Measurement:

An IBM personal computer was interfaced to the analogue outputs of a DVM, an electrometer and a lock-in amplifier via a A/D converter (Tecmar Labmaster) for acquiring and recording data on solar cell parameters. A program allowed the acquisition of data simultaneously from three channels to be saved on a diskette. When provided with the frequency, area of the sample and a.c. voltage across the sample, $1/C^2$ was calculated by the program, where C is the measured capacity between the silicon and the evaporated aluminum. It also enabled the plotting of $1/C^2$ versus V and I versus V sequentially on an HP plotter. The voltage V was ramped from -1 to 1 volt with a 100 second period for I-V measurement and the a.c. voltage across the sample was adjusted to 5 mv at 100 kHz for the capacity measurement.

For capacity measurement, the lock-in-amplifier measured the out of phase component across the samples. The lock-in-amplifier was zeroed in phase with a resistance placed instead of the sample; this was done at a sensitivity of 10 μ V full scale. The lock-in-amplifier was adjusted to 90⁰ out of phase and to a suitable scale to take the measurement of the cell capacity. Fig.2-5 shows a schematic diagram of the electrical circuit.

The shunt resistance was obtained from a least square fit of the reverse biased portion of the I-V curve. The reverse saturation current I_0 was obtained by plotting $\ln I$ versus V.

Assuming equation 4.2 then from the straight line one obtains $\ln I_0$ to be equal to the slope of the line multiplied by the y-axis intercept plus 1.

2.2.3. Interpretation of Capacity measurement:

The solar cell is thought of as an RC parallel circuit. This is justified by choosing a high enough frequency to enable one to ignore the inversion layer, oxide and surface state capacitances. To estimate the capacitance contribution by the inversion layer we use the expression derived by Barbottin et al.³⁹

$$V_{inv} = (-2KT/q) \ln N_A/n_i \quad (2.1)$$

$$W_{scr} = (2e_s/qN_A |V_{inv}|)^{1/2} \quad (2.2)$$

$$e_s = k_s e_0 \quad (2.3)$$

V_{inv} is the voltage needed to invert the surface, N_A is the acceptor density, n_i is the intrinsic carrier density, W_{scr} is the width of the space charge layer including the inverted region, kT/q has the standard meaning, e_0 permittivity of vacuum, e_s permittivity of Si and k_s dielectric constant of Si.

For the undamaged solar cells V_{fb} (flat band potential or the band bending) has been experimentally found to be greater than V_{inv} ^{33,40}. However, the magnitude of the thickness of the inverted layer is much smaller than W_{scr} as given above.

Furthermore, the oxide thickness is such that electrons can tunnel in both directions through the insulator layer^{41,1} that implies that due to the tunnel current the minority carrier quasi-fermi level is pinned to the metal fermi level³³. An increment in the applied bias will mainly appear as an increment of the width of the space charge region⁴². The oxide capacitance can be ignored because it is so thin. The oxide capacitance per unit area

$$C_{ox} = \epsilon_{ox} / d \quad (2.4)$$

where d is the thickness of oxide approximately 20 Å and ϵ_{ox} is the permittivity of SiO₂ ($3.9\epsilon_0$). The capacitance of the space charge region per unit area

$$C_{scr} = \epsilon_s / W_{scr} \quad (2.5)$$

where ϵ_s is the permittivity ($11.9\epsilon_0$) and W_{scr} a few thousand angstroms. At the higher frequency of capacitance measurement C_{ox} should be negligible compared to C_{scr} .

Surface state capacitance can be ignored at high frequency because there is a resistor in series with this capacitor. Surface states which have a resistance R_s and capacitance C_s would have a lifetime $t_s = R_s C_s$. If a frequency f is chosen greater than $1/t_s$ then the surface state effect would be negligible.

With these approximations the differential capacitance of

the solar cell per unit area (similar to n+p junction) would be given by Ref.2

$$C=dQ/dV=[qe_s N_A/2((V_{fb}-V-KT/q))]^{1/2} \quad (2.6)$$

V is the applied voltage. A plot of $1/C^2$ versus applied voltage gives a straight line the slope of which is inversely proportional to N_A , the intercept with the x-axis is $-V_{fb}+kT/q$.

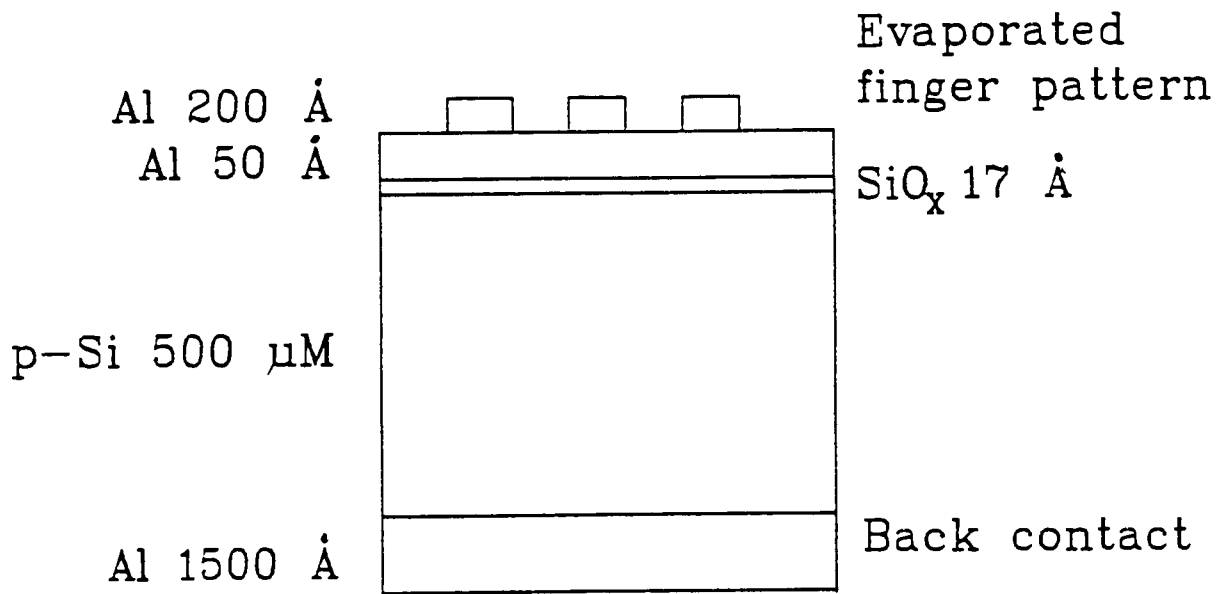


Fig 2-1 The MIS solar cell sturcture

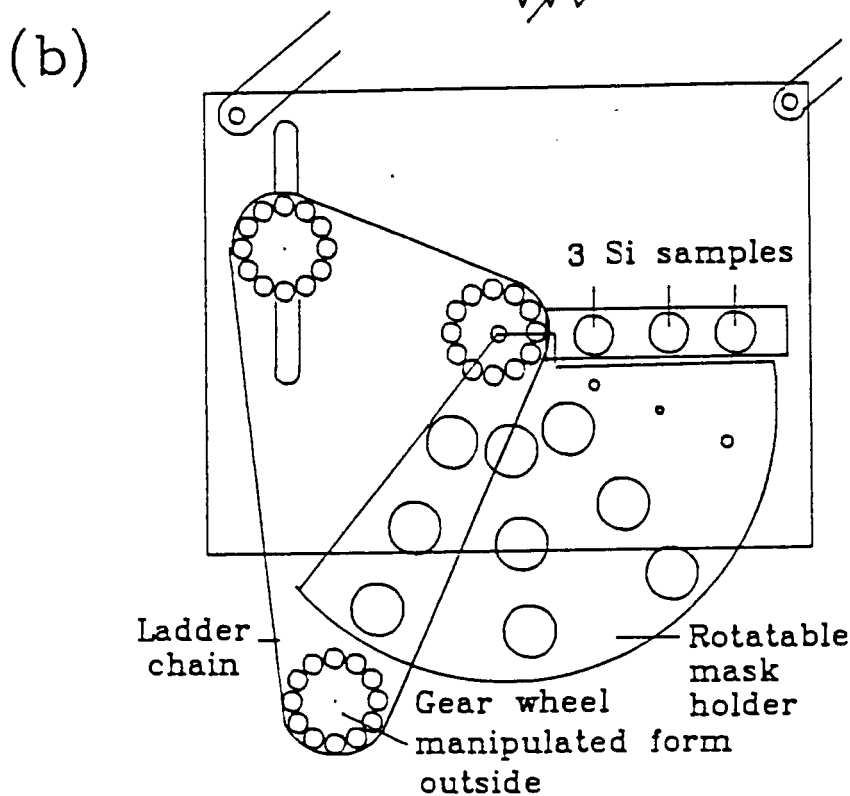
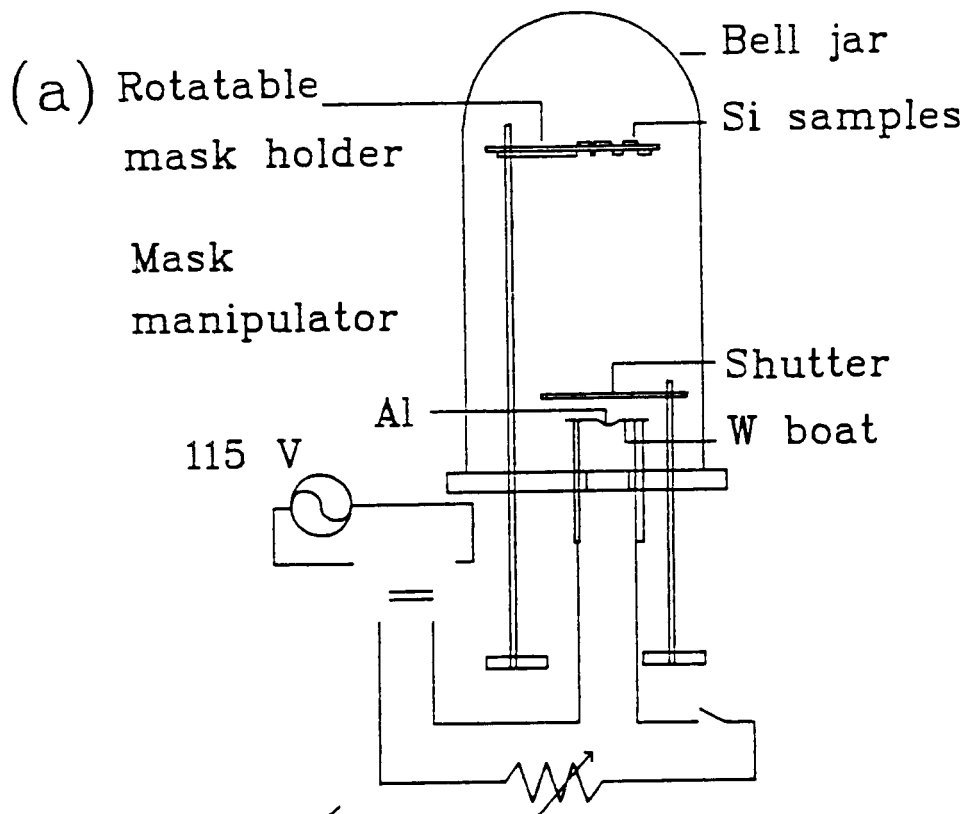


Fig.2-2 (a) Schematic diagram of the vacuum evaporator

(b) The rotatable mask holder

TO VACUUM PUMP

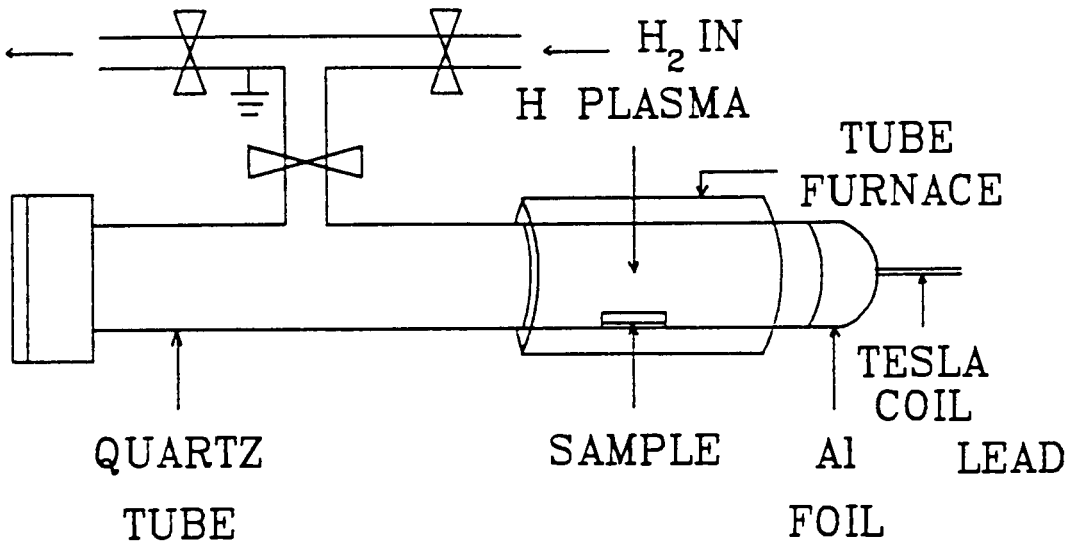


Fig 2-3 Hydrogen passivation apparatus

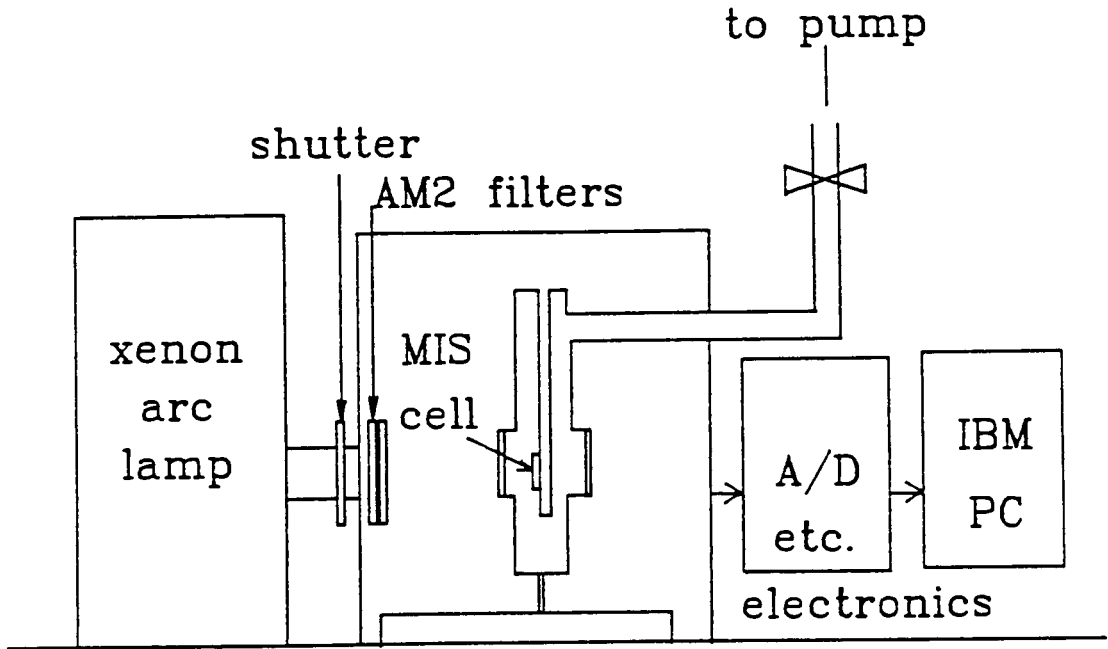


Fig 2-4 Measuring device for the solar cell characteristics

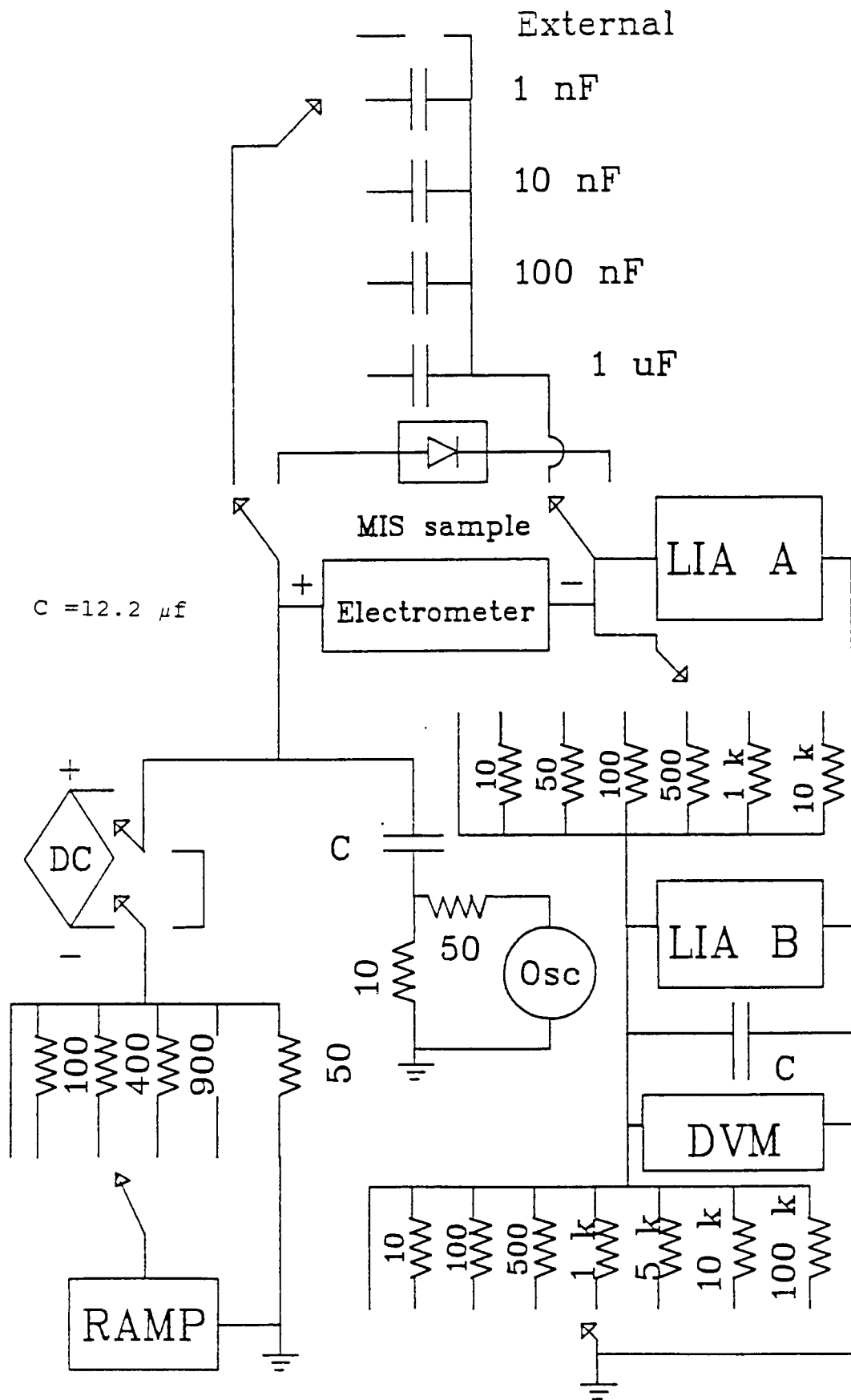


Fig 2-5 The electrical circuit used in measuring I/V and C/V

Chapter III

3. Experimental results:

The experimental results are summarized in Tables I and II. Table I is for undamaged samples, each entry representing an average of at least five samples. Table II is for damaged samples, with an extra entry for the "shunt resistance". The shunt resistance is the value of dV/dI taken before the forward bias region. A second measurement of these samples was taken; for some this was done a few days after the first measurement, for others after a few months. This is written in a lower row in both tables.

3.1. Undamaged substrate:

Silicon was subjected to treatment in a hydrogen plasma for various exposure times. This has led to changes in the parameters of the solar cells subsequently fabricated from this silicon. The untreated solar cell parameters are $V_{oc} = 430 \pm 20$ mv, $J_{sc} = 11.4 \pm 0.6$ mA/cm², FF = 70 ± 2.5 % and efficiency = 3.5 ± 0.2 . Table I records how these parameters degraded with plasma treatment. Figures 3-1 to 3-5 show graphically how the various important parameters vary as a function of hydrogen treatment, the dotted lines showing the results with the plasma not ignited, the solid lines showing the observations after plasma treatment.

3.1.1 The effect of a hydrogen plasma on solar cell parameters:

The open circuit voltage does not seem to be affected by a hydrogen plasma except after a long period of exposure. Although there is scatter, as observed in Figure 3-1, it is probably due to some non-reproducibility in the preparation; for example in the evaporator one did not consistently get the same quality of the vacuum during the deposition of the back contact. After a long period of exposure to the plasma ($3\frac{1}{2}$ hours), the open circuit voltage drops to 320 ± 20 mv.

As observed in Figure 3-2, the short circuit current density J_{sc} shows no significant change on average for 5, 10 or 20 min of exposure to the hydrogen plasma. With 40 minutes exposure the current drops quite suddenly to 4.0 ± 2.5 mA/cm², then J_{sc} drops again for 80 minutes and $3\frac{1}{2}$ hours of exposure to 1.7 ± 0.1 and 1.4 ± 0.2 mA/cm² respectively.

The fill factor (Figure 3-3) appears to drop with hydrogen atom exposure from an average of 73 ± 1 % for 5 minutes of passivation to 58 ± 2 % for 20 minutes of passivation, then it improves for 40 minutes and 80 minutes of passivation to 72 ± 4 and 73 ± 2 % respectively. (We note that this is the interval where I_{sc} goes down rapidly). After $3\frac{1}{2}$ hours of plasma treatment again the FF deteriorates to 61 ± 7 %.

The efficiency (Figure 3-4) is not affected for the 5 and 10 minutes treatment in H plasma. It starts dropping rapidly with a longer duration of exposure. For $3\frac{1}{2}$ hours exposure it reaches 0.3 ± 0.1 %.

The carrier density is affected the most by exposure to the

hydrogen plasma, as shown in Figure 3-5. Even after 5 min of treatment N_A drops from an average of 11.5 to $10.3 \times 10^{14} / \text{cm}^3$ and drops further by about two orders of magnitude for the $3\frac{1}{2}$ hours plasma treatment.

In summary, the hydrogen plasma treatment seems to lower the density of charge carriers for all exposure times, the efficiency degrades rapidly after 20 minutes, the short circuit current degrades after 40 minutes, and the open circuit voltage degrades only slightly and then only after $3\frac{1}{2}$ hours exposure time. The fill factor begins to degrade with 10 minutes exposure, then recovers, degrading again finally with $3\frac{1}{2}$ hours exposure to the plasma. Thus for these undamaged samples, the solar cell characteristics in general degrade with hydrogen plasma treatment.

3.1.2. Stability of the characteristics after plasma treatment:

It was considered important to determine whether the effects of the hydrogen plasma in undamaged samples were permanent or whether heat treatment would return the samples to the better parameters. The concept of course is that hydrogen enters the silicon, and the question is whether it will out-diffuse under heat treatment. However, during the normal processing of the samples yielding the parameters above, there was ample opportunity for hydrogen out-diffusion. Some of the samples were only exposed for 5 minutes to a hydrogen plasma, then were heated at approximately 380°C in H_2 for the rest of the 3 hours, the last $\frac{1}{2}$ hour heater was switched off. Furthermore,

the samples were heated again for 15 min at a temperature above 500 °C to anneal the Al back contact and build an oxide. The 500 °C treatment was part of the solar cell fabrication process. Despite the heating of the samples there was still a noticeable decrease in the number of charge carriers. The second measurement of the samples gave an indication that the effect of passivation was still noticeable after a significant time interval. All cells seem to degrade with time, except, for the samples passivated for 3½ hours there was an improvement in the open circuit voltage and the fill factor. One concludes from this that some hydrogen must have either evolved, that which was not at stable lattice sites, or that hydrogen atoms may have recombined to form molecules that are electrically neutral.

3.1.3. The effect of molecular hydrogen:

The solar cells do not seem to be affected by heating for 3 hours at approximately 380 °C in molecular hydrogen (Pressure≈20 mtorr). Although the fill factor appears to degrade from the untreated value of 70% to an average value of 61 %, the samples that were done identically except were not treated in molecular hydrogen also develop a low fill factor (65 %), suggesting the heat treatment may have affected the samples slightly.

3.2. Solar cells with surface dislocation loops:

The standard treatment described in section 2.1.5, where 1 μm Al₂O₃ grit was used to produce surface dislocation loops, was found to degrade the solar cell performance substantially to

$V_{oc} = 99 \pm 11$ mv, $J_{sc} = 7.4 \pm 0.9$ mA/cm², FF= 29±1 %, and efficiency= 0.21±0.05 %. This is consistent with earlier studies (Ref.33). The following subsections show how hydrogen treatment passivates the degradation from the dislocations, improving the solar cell performance. Table II shows the observed averages; Figure 3-6 shows typical I/V curves for with and without the damage treatment, both in the dark and under illumination. It is noted that a significant dark reverse current appears when the sample is "damaged". Figure 3-7 shows the effect of hydrogen passivation on the photoresponse, Figure 3-8 shows the effect of hydrogen passivation on the dark response of the solar cells. We note that the dark reverse current is minimized by the hydrogen treatment.

3.2.1. Effect of the hydrogen plasma:

All damaged samples are exposed to the plasma for 3 hour at temperature approximately 380 °C and left to cool in the plasma for 1/2 hour. Some are done under a better vacuum (Pressure approximately 10⁻⁶ torr). These samples will be referred to as type 1. Type 2, on the other hand were passivated in a system which was not evacuated to as low a pressure (Pressure approximately 10⁻⁵ torr), and it is believed there may be a significant partial pressure of H₂O in the latter case.

Type 1 samples show improvement in the V_{oc} after the 3½ hours exposure from less than 10 mv to an average of 240±30 mv. Furthermore, the current density improves to quite a high value of 10.8±1.5 mA/cm², almost the same value of the undamaged solar

cells. The FF also shows some improvement to 37.7 ± 4.2 %. The efficiency rises from 0.21 ± 0.05 % to an average of 1.0 ± 0.3 %.

On the other hand, type 2 samples show a much greater improvement for the V_{oc} , which reaches 418 ± 14 mv, very close to the undamaged value. However, the photocurrent density drops to 2.6 ± 0.3 mA/cm² compared to the value for untreated samples of 7.4 ± 0.8 mA/cm². The FF improves markedly to 71 ± 3 % from 29%. For these samples, the efficiency is higher than damaged untreated samples, their efficiency averages 0.8 ± 0.1 %, but this is lower than the efficiency for type 1 samples. Figure 3-7 shows typical curves for treated samples of both type 1 and type 2.

In summary, the hydrogen plasma treatment led to an overall improvement in the solar cell parameters of type 2 samples, except for the short circuit current.

3.2.2. Effect of molecular hydrogen:

Samples heated in molecular hydrogen showed no noticeable change in most of the solar cell parameters, as observed in Table II, but there is an obvious improvement in the dark reverse saturation current. It drops by almost an order of magnitude from 1.41×10^{-4} to 6.06×10^{-5} mA. The "shunt resistance" correspondingly improves, from an average of $2.15 \pm 0.99 \times 10^3$ ohms for untreated samples to $16.3 \pm 8.2 \times 10^3$ ohms for H₂ treatment samples. However, this is not as great an improvement as for the plasma treatments where R_{sh} for type 1 samples is 1.04×10^6 ohms and type 2 samples 1.4×10^5 ohms.

3.2.3. Stability of passivation of molecular hydrogen and hydrogen plasma treatments:

As mentioned previously samples are heated for 15 minutes during the solar cell fabrication to build a surface oxide and anneal the back contact. Although, the temperature is above 500 °C the effect of molecular and atomic hydrogen could still be detected on the solar cell parameters including those parameters affected by the dislocations especially for type 2 where the effect of dislocation on open circuit voltage has been rendered negligible. We have however done no systematic studies of stability.

Solar Cell Parameters on Undamaged Silicon. For each entry there are two values, first representing the parameter immediately after preparation of the solar cell, the second several weeks after. Cells were exposed to plasma for different durations as low as 5 minutes and up to $3\frac{1}{2}$ hours.

TABLE I Undamaged Solar Cell Parameters

	V_{oc} mv	I_{sc} mamp	FF %	EFF	N_A /cm ³
No treatment	430±20	4.3±0.2	70±3	3.5±0.2	11.5±0.3 10 ¹⁴
	410±20	4.5±0.4	66±2	3.1±0.3	11.6±1.4 10 ¹⁴
5 minutes	450±10	3.7±0.2	73±1	3.1±0.2	10.3±0.6 10 ¹⁴
	420±20	4.4±0.3	63±7	3.1±0.5	9.6±0.6 10 ¹⁴
10 minutes	460±20	4.4±0.2	64±3	3.4±0.2	5.4±2.1 10 ¹⁴
	400±20	5.2±0.3	59±1	3.2±0.3	6.3±1.7 10 ¹⁴
20 minutes	420±10	4.2±0.6	58±3	2.7±0.4	5.2±1.9 10 ¹⁴
	400±10	4.2±0.6	55±4	2.5±0.4	6.0±1.9 10 ¹⁴
40 minutes	440±20	1.5±1	72±4	1.2±0.6	2.0±2.5 10 ¹³
	440±30	1.7±1.2	70±4	1.3±0.6	15±25 10 ¹³
80 minutes	410±10	0.6±0.1	73±2	0.5±0.1	1.6±0.4 10 ¹³
	400±10	0.6±0.1	73±1	0.5±0.1	6.9±5.7 10 ¹³
210 minutes	320±50	0.5±0.1	61±7	0.3±0.1	3.6±2.3 10 ¹³
	350±20	0.7±0.1	63±7	0.4±0.1	5.8±0.5 10 ¹³
Molecular	410±20	4.2±0.3	61±7	2.8±0.4	11.9±2.2 10 ¹⁴
Hydrogen	370±30	5.0±0.3	52±9	2.6±0.6	9.2±0.8 10 ¹⁴

Solar Cell Parameters on Damaged Silicon. For each entry there are two values, first representing the parameters immediately after preparation of the solar cell, the second several weeks after. Type I and Type II were treated in hydrogen plasma for 3½ hours, however the passivation tube was evacuated to $P \approx 10^{-6}$ torr for Type I and $P \approx 10^{-5}$ torr for Type II before it was back filled with hydrogen.

TABLE II

Damaged Solar Cell Parameters

	V_{oc} mv	I_{sc} mamp	FF %	EFF%	R_{sh} kohm	N_a cm^{-3}
No treatment	99±11	2.8±0.3	29±1	0.21±0.05	2.2±1	14±2 E14
	78±9	1.4±0.4	27±1	0.08±0.03	1.9±1.1	11.1±1.1 E14
Type I	238±33	4.0±.6	38±4	1.01±0.32	1045±1132	5.6±1.1 E14
	206±37	3.2±0.9	33±4	0.62±0.29	54.3±62.2	5.5±0.7 E14
Type II	418±14	1±0.1	71±3	0.76±0.12	140±42	0.9±0.4 E13
	388±25	1±0.2	65±8	0.66±0.15	140±101	3.4±1.3 E13
Molecular H ₂	112±29	1.9±0.7	29±2	0.18±0.09	16.3±8.2	7.9±0.3 E14
	86±32	1.2±0.7	27±2	0.09±0.08	11.1±6.2	7.4±2.9 E14

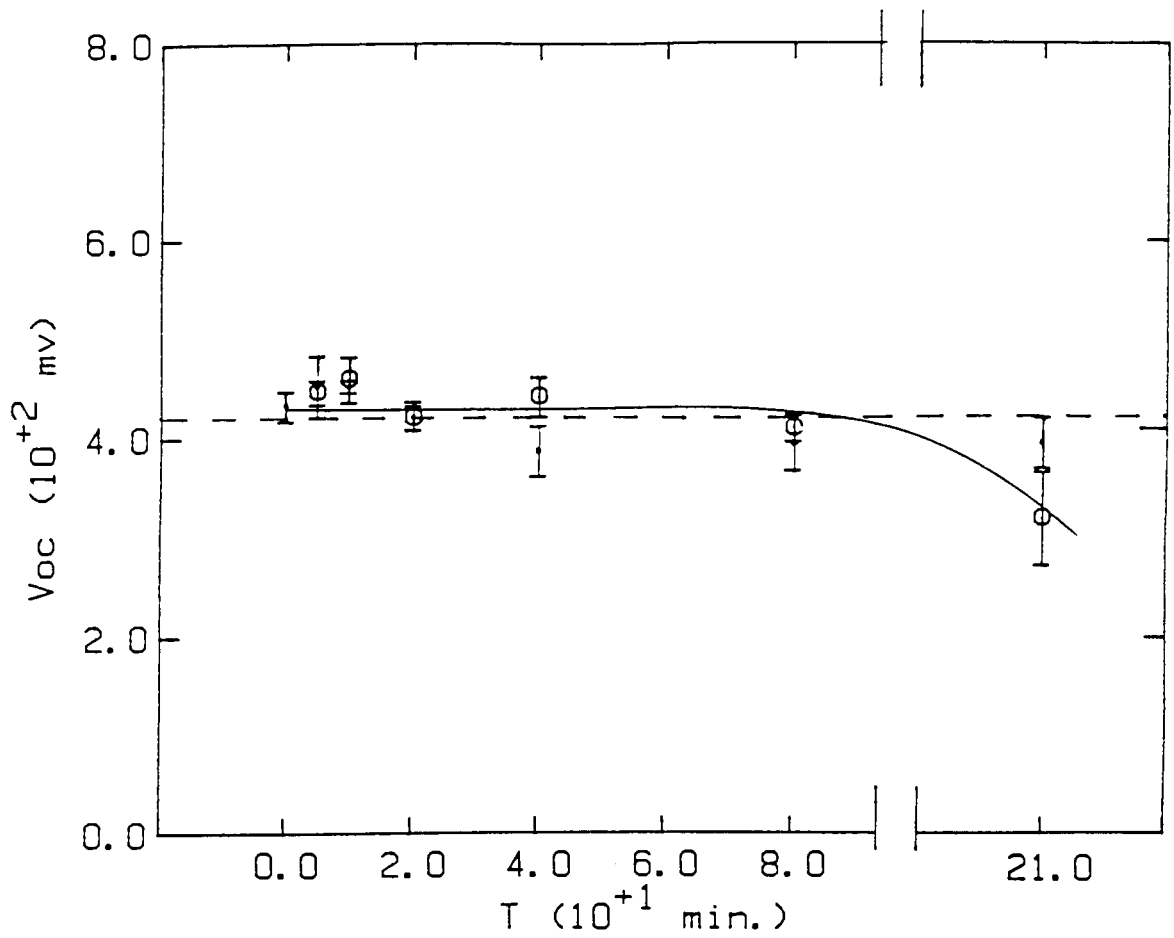


Fig 3-1 The variation of open circuit voltage with passivation time. The circles are measurements on passivated samples, the dots are untreated ones.

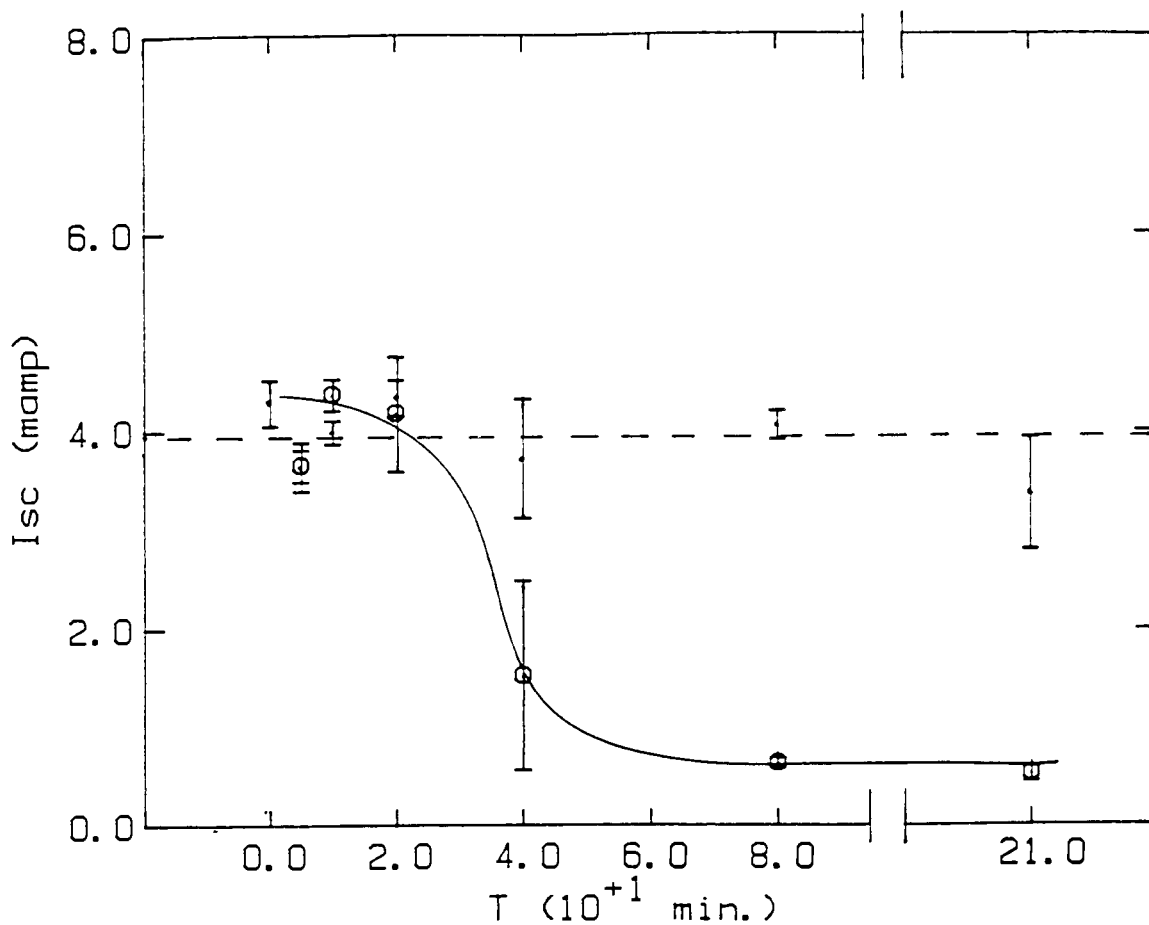


Fig 3-2 The variation of the short circuit current with passivation time. The circles are measurements on passivated samples, the dots are untreated ones.

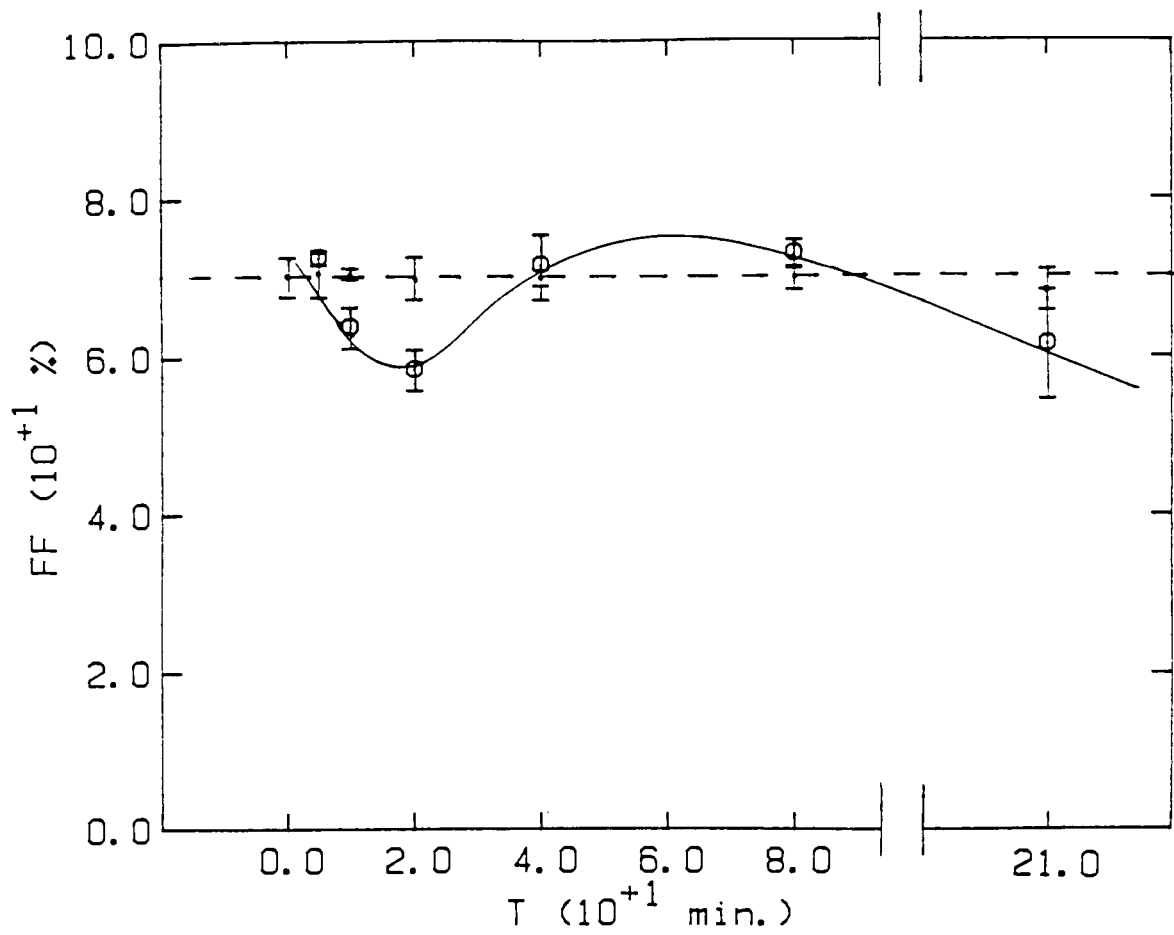


Fig 3-3 The variation of the Fill Factor with passivation time. The circles are measurements on passivated samples, the dots are untreated ones.

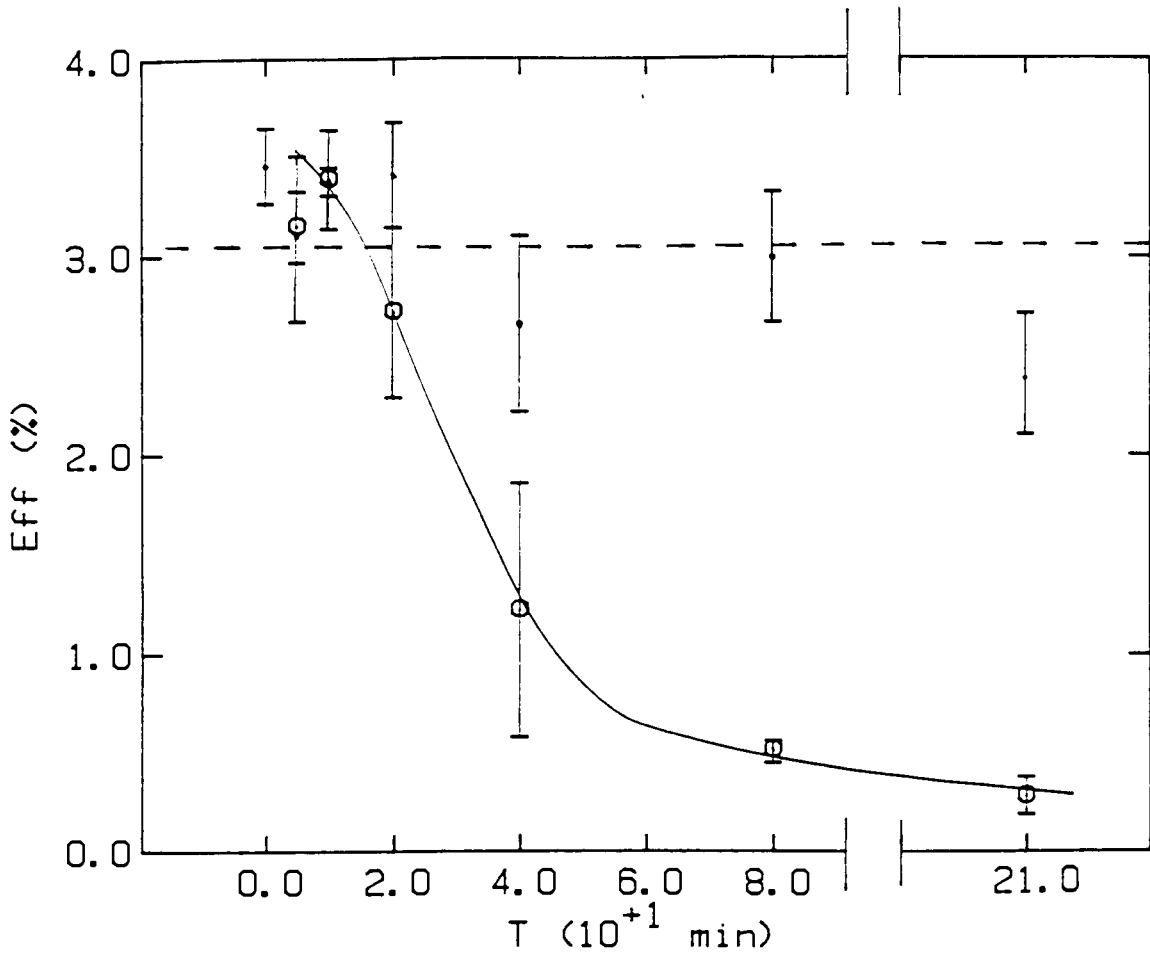


Fig 3-4 The variation of the Efficiency with passivation time. The circles are measurements on passivated samples, the dots are untreated ones.

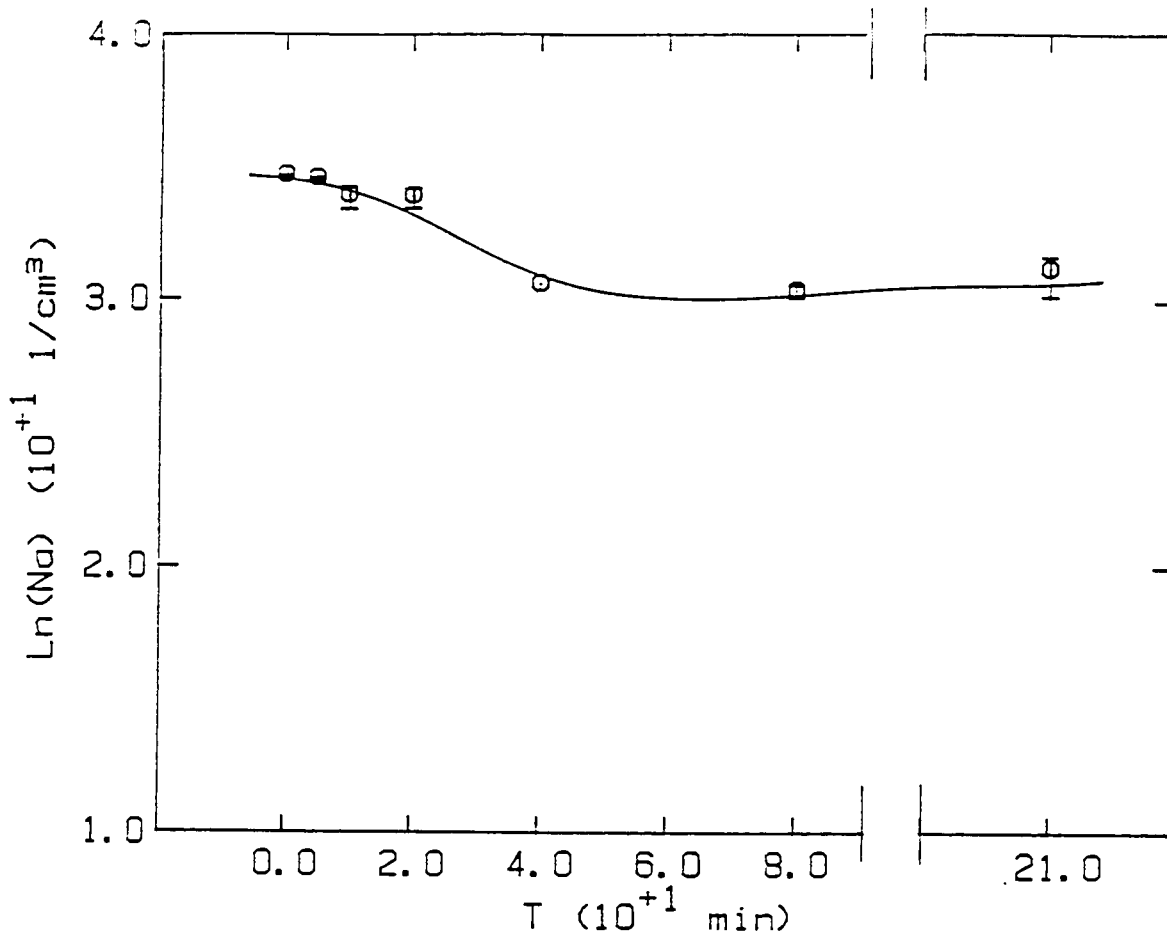


Fig 3-5 The variation of the Number of charge carriers with passivation time.

The error bar for samples passivated for 40 minutes is not included in the graph.

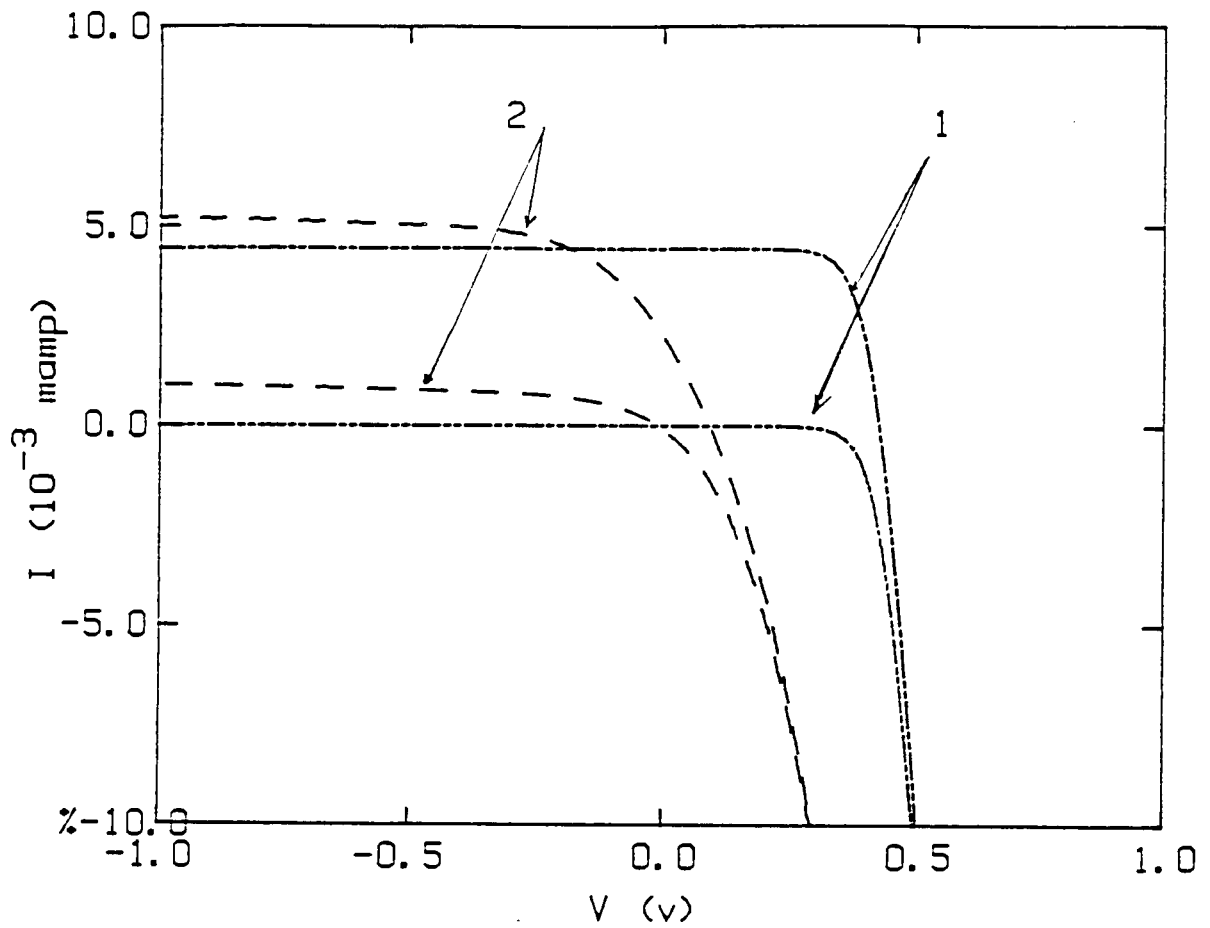


Fig 3-6 The I-V characteristics of solar cells in the dark and under illumination,
 1. For undamaged samples.
 2. For damaged samples.

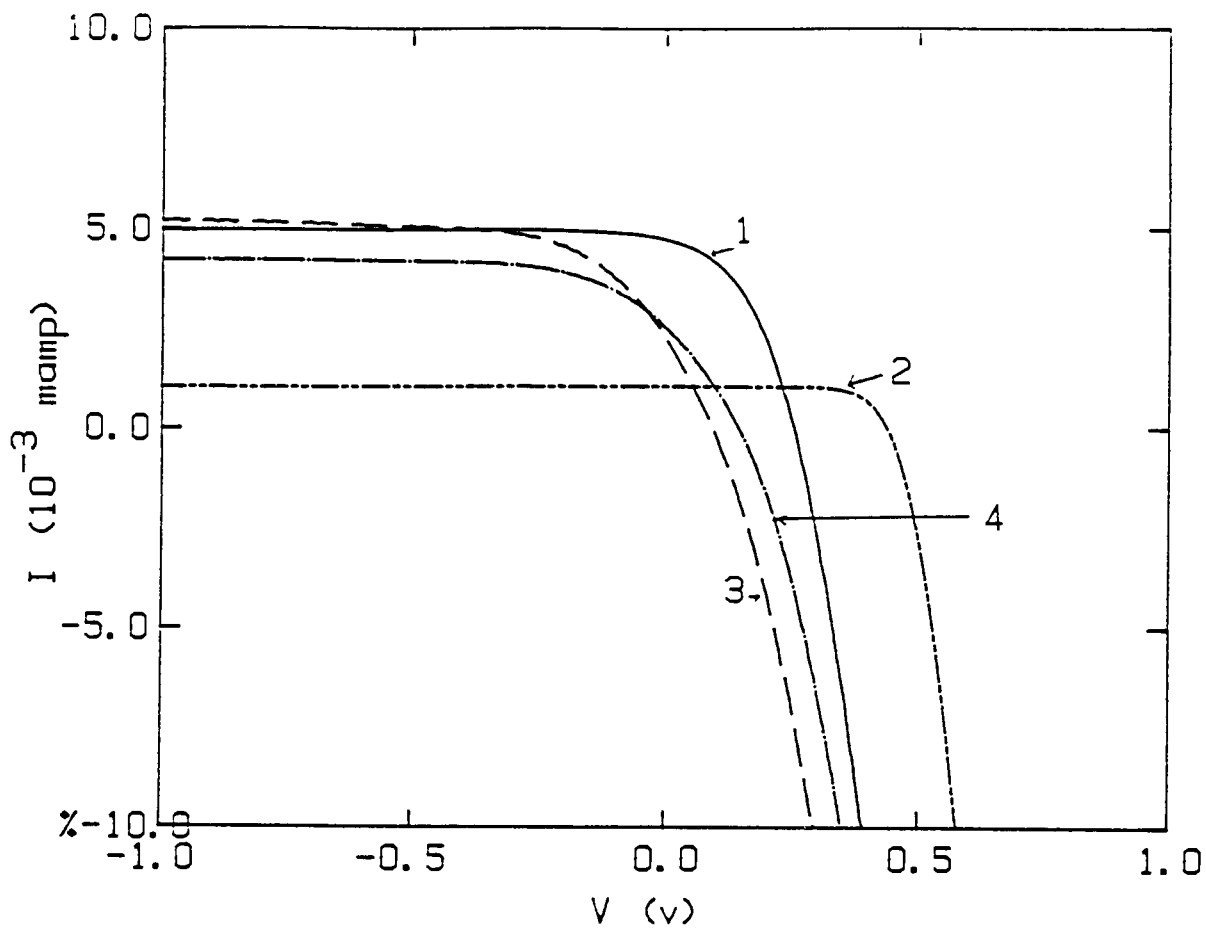


Fig 3-7 Damaged samples I-V characteristics under illumination,

1. Type I H plasma treated (system lowest pressure 10^{-6} torr).
2. Type II H plasma treated (system lowest pressure 10^{-5} torr).
3. No hydrogen treatment.
4. Molecular hydrogen treatment.

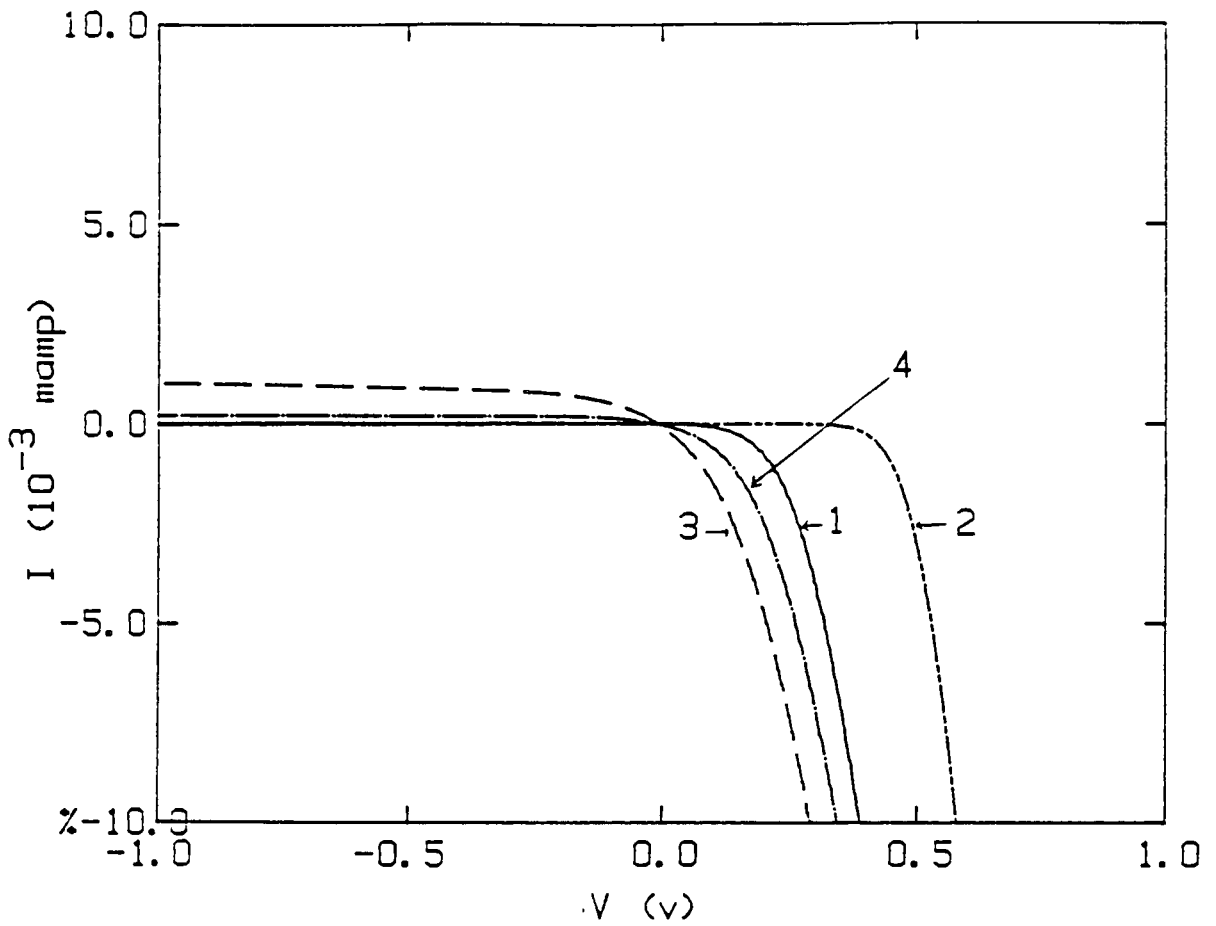


Fig 3-8 Damaged samples I-V characteristics in the dark.

1. Type I H plasma treated (system lowest pressure 10^{-6} torr).
2. Type II H plasma treated (system lowest pressure 10^{-5} torr).
3. No hydrogen treatment.
4. Molecular hydrogen treatment.

Chapter IV

4. Discussion and Conclusion:

4.1.1. Undamaged samples:

The major effect of the hydrogen plasma treatment of undamaged samples is the lowering of N_A , which has been observed by many authors (refs 7,28,43). N_A is obtained from C-V curves equation 2.6 and (Fig.4-1, 4-2). The C-V curves for samples subjected to longer periods of plasma (40 minutes and above) were hard to interpret. A least square fit was done on that part of the curve where the voltage was ramped in the forward direction from -1 to 1 v and the other part of the curve was ignored.

The MIS behaves as an n^+p junction the dark current is ideally a diffusion current (ref.1)

$$I = qn_i^2 D_n / N_A L_n (\exp qV/nkT - 1) \quad (4.1)$$

where D_n is the diffusion coefficient, L_n is the minority carrier diffusion length, and n is the ideality factor.

According to Corbett et al. (ref. 43) hydrogen diffuses as a positive and neutral species in p-type silicon. It passivates impurities and neutralizes shallow acceptors. The hydrogen has a much higher concentration near the surface; the concentration drops deeper into the sample. Using deuterium for passivation they found that its concentration at the surface was of the order of 10^{20} cm^{-3} . In a study by Pankove et al. (ref. 44) 99%

of the acceptors were passivated, and when the resistance was measured it was higher at the surface than deeper into the sample, and the magnitude of the resistance increased proportionally with treatment time.

It may then be concluded that in our case also hydrogen atom exposure can render the boron at the surface completely neutral and a silicon hydride layer may be created effectively creating an insulator layer which, when added to the thickness of the oxide, might lead to the suppression of the photocurrent. In the book by Pulfrey (ref.1) thicker oxides suppress the photocurrent.

Passivation of boron near the surface leads to a high resistance and this means a higher n , where n is the diode ideality factor. Furthermore, if a small amount of hydrogen were to diffuse into the sample and passivate deep level impurities then that may lead to a longer lifetime for the minority carriers and an improvement in I_0 ($I_{diff} + I_{rec}$) section 1.1. Thus, there is a drop in the photocurrent without a noticeable drop in the open circuit voltage, V_{oc} , given by²

$$V_{oc} = nkT/q \ln(I_{sc}/I_0 + 1) \quad (4.2)$$

However, for longer periods of plasma exposure, for example $3\frac{1}{2}$ hours, the hydrogen penetrates deeper into the sample possibly beyond the space charge layer in high concentration, leading to lower N_A and higher diffusion currents. That would lower the open circuit voltage.

Fill Factor: The behaviour of the fill factor, first degrading then recovering (Fig.3-3), was unexpected. If there

is change in the surface layer such as the formation of an insulator layer, then that could explain the initial lowering of the FF that is observed in Figure 3-3 up to 40 minutes exposure. However, for intermediate exposure time, 40 and 80 minutes, the FF improves. We suspect that this improvement could be an artifact associated with the rapid lowering of the short circuit current after 40 minutes exposure. The sudden lowering of I_{sc} makes the fill factor apparently improve. With $3\frac{1}{2}$ hours exposure to plasma the fill factor decreases again. This could be because hydrogen penetrates deeper into the sample, passivating N_A , and causing the resistivity of the substrate to increase thus V_{oc} decreases, samples of lower doping have smaller V_{oc} ^{1,45}. Alternately the FF could degrade by further surface damage.

Efficiency: The efficiency is affected most by the drop in J_{sc} , dropping to its lowest value of 0.3 ± 0.1 % after $3\frac{1}{2}$ hours exposure to the plasma (Fig.3-4). Efficiency also is affected by the FF, so although J_{sc} does not show any significant change until the sample is treated for 40 minutes the efficiency begins to drop at lower exposure time because the fill factor drops.

As mentioned hydrogen plasma treatment of the undamaged solar cell seems mainly to reduce the density of charge carriers. This is to be expected, according to refs. 28 and 43 where it is shown that the hydrogen enters the silicon and interacts with acceptors, rendering them neutral impurities. The more hydrogen introduced into the samples the deeper the neutralization of the acceptors, leading to lower photocurrent.

With longer times of plasma exposure the open circuit voltage seems to be affected. Too much hydrogen leads to the degradation of all solar cell parameters. Thus it would appear, considering these results only, that a hydrogen treatment is undesirable for MIS solar cells from single crystal p-type silicon.

Stability: taking a second measurement of the samples, some of which were taken a few months (up to 8 months) after the first one, still showed the carrier concentration to be lower, leading one to conclude that hydrogen is stable in the solar cell at room temperature. We also found that heating the samples in argon and oxygen to temperatures above 500 °C for 15 minutes, a standard treatment, was unable to drive the hydrogen completely out of the sample.

4.1.2. Damaged samples:

When dislocations are introduced into the silicon majority charge carriers are trapped at the dislocation creating a potential barrier. The more charges trapped the higher the barrier. The minority carriers are attracted to and will recombine at the dislocations. From paper by Glaenzer et al. (ref.36) he found that dislocations in p-type Si create donor levels in the energy gap.

When the damaged samples are exposed to a hydrogen plasma presumably the hydrogen atoms diffuse in or to the dislocations bonding to the silicon dangling bonds. From the literature H has a much higher diffusion constant for the GB and dislocations

than through the bulk silicon. As is observed with interface states, the deep levels may disappear, the hydrogen rendering them ineffective as hole traps. Thus hydrogen passivation may lead to the lowering of the potential barrier. Fig.4-3 shows the effect of a lower barrier from the model³³, and this agrees with the experimental results for type 1 samples.

Initially, then, the plasma treatment will lead to an improvement in the solar cell parameters, a higher I_{sc} , V_{oc} , FF and efficiency as the hydrogen acts to negate the effect of the dislocation. This behaviour is realized in type 1 samples as an overall improvement.

Passivation of dangling bonds at the dislocation however, also means that the shunting due to dislocations is reduced. Experimentally on average this is observed (table II), however there is a large scatter. Although samples are heated for 15 minutes at temperature above 500 °C they still retain the effect of passivation.

When too much H ions are formed in the plasma, in type 2 samples, more hydrogen will diffuse through the bulk. As described above, for undamaged silicon passivation the boron atoms are neutralized leading to the creation of an insulator region (silicon hydride) at the surface which in turn leads to a drop in the photocurrent and the short circuit current. Naturally this same decrease in J_{sc} with long exposure is observed with damaged samples. The "shunt resistance" is quite high leading to a large improvement in the open circuit voltage, which almost reaches that of the undamaged samples. For a long

time the effect of plasma treatment on the short circuit current was not noticed in experiments on polycrystalline Si solar cells. For example Robinson⁵ commented that J_{sc} was not significantly affected by hydrogen treatment.

We have also found molecular hydrogen does affect damaged silicon. Heating the damaged Si in molecular hydrogen at 380 °C leads to a noticeable improvement in the dark reverse saturation current I_0 and the R_{sh} . Molecular H_2 has a positive effect, as observed by Sardi et al. (ref.31), as is supported by a theoretical calculation which suggests H molecules may possibly enter strained Si-Si bonds and would tend to stabilize the bonds over a range of bond length.⁴⁶ Our results suggest that molecular hydrogen can diffuse to some extent along dislocations, providing passivation but only atomic hydrogen can reach the bulk to interact with acceptors.

Stability: Solar cells that were measured for a second time showed degradation for most parameters. However the degradation was systematic, type 1, presumably with less hydrogen, still has lower V_{oc} and higher I_{sc} compared to type 2. N_A remains higher for type 1.

4.2.Conclusions:

There seem to be a consensus between theoreticians and experimentalists about the position of the neutralizing hydrogen in the lattice (ref. 47,48,49,50). The model proposed by Pankove et al.(ref.51); is that the passivating hydrogen exists in a position between the silicon and boron atoms causing the

boron atoms to relax from their substitutional position and lose their acceptor character. However, there is still no clear model on how hydrogen diffuses into the crystal and the other positions the hydrogen may occupy. Furthermore, there is no agreed-upon value for the activation and the dissociation energies (ref. 7,8,4). Johnson et al. (ref.52) state that there is no direct experimental evidence for the existence of H_2 in crystalline Si.

Hydrogen plasma treatment of damaged solar cells has some advantages as well as some disadvantages. The disadvantage is that excess exposure to plasma has proven to decrease the charge carrier concentration (holes) and lower the short circuit current and this affects the solar cell efficiency. In other words the acceptors are "passivated". If too much hydrogen is incorporated that may also lead to a drop in the open circuit voltage. On the other hand, the advantage is that in damaged samples a moderate plasma exposure leads to an overall improvement in the cell parameters, for the degrading effect of dislocations is minimized. However, the passivation of dangling bonds at dislocations is not complete: V_{oc} does not recover totally but the I_{sc} recovers to a satisfactory value. With extensive plasma exposure when too much hydrogen is incorporated the dislocations appear to be completely passivated. With no shunting current through the dislocation I_0 drops, causing a substantial improvement in the V_{oc} . However, an insulating layer may be created at the surface suppressing the photocurrent as is observed with undamaged Si.

We believe this is the first time this competitive effect has been recognized, and it is clear that before hydrogen passivation of "practical" (in the sense of using low cost low grade polycrystalline silicon) solar cells will be useful, the effect must be controlled.

Further experiments should be carried out to optimize the amount of hydrogen entering the sample. This is helped by the fact that hydrogen seems to diffuse more readily in the dislocation than in the bulk of the semiconductor. A method may be devised to selectively introduce hydrogen in the GB's or dislocations. Experiments must still be done to test the stability of the hydrogen in the silicon, how it diffuses and how molecules are formed.

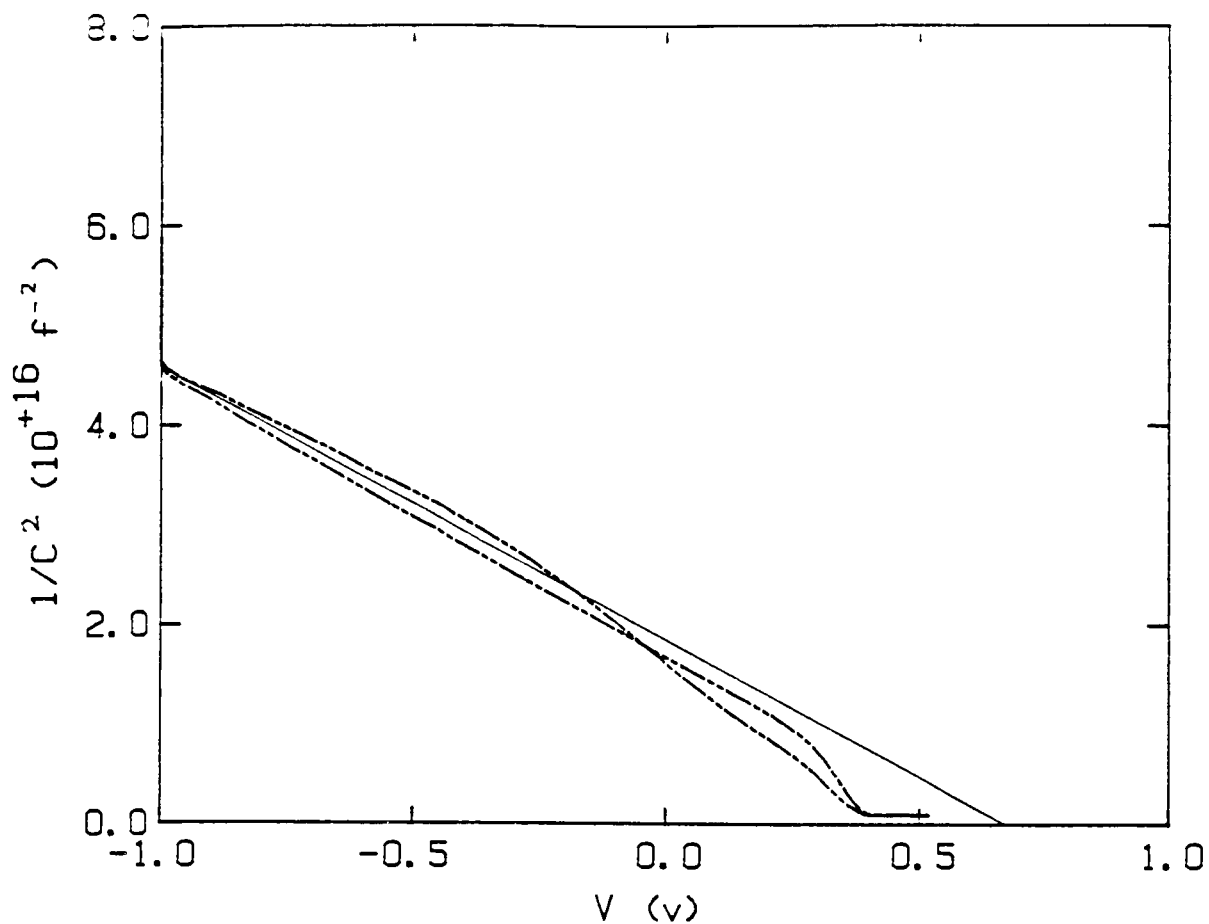


Fig 4-1 The variation of $1/C^2$ with the voltage for undamaged samples and no hydrogen treatment. The dotted line is $1/C^2$ versus V from -1 to 1 volt and back. The solid line is a least square fit to calculate N_A .

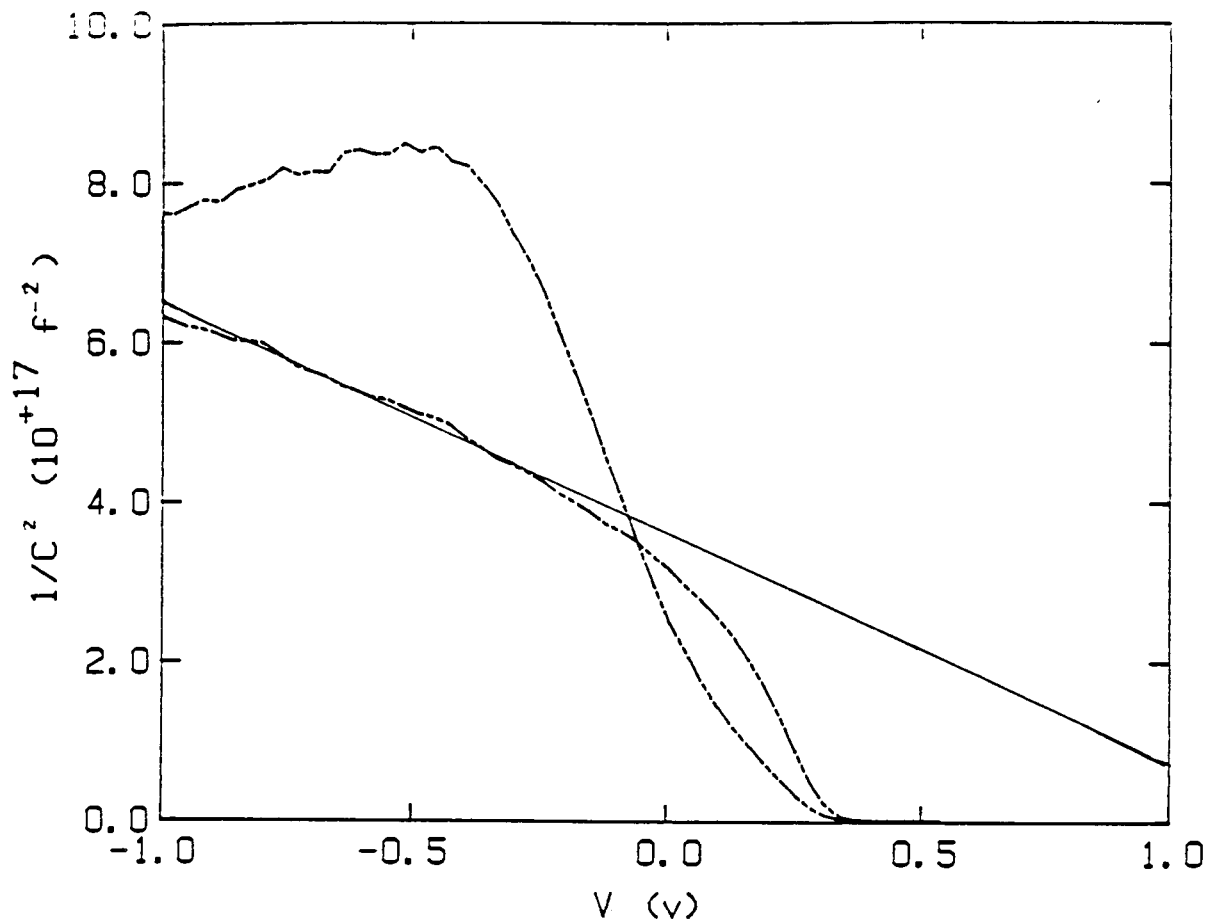


Fig 4-2 The variation of $1/C^2$ with the voltage for undamaged samples with $3\frac{1}{2}$ hours hydrogen plasma treatment. The dotted line is $1/C^2$ versus V from -1 to 1 volt and back. The solid line is a least square fit to calculate N_A when the voltage is ramped from reverse bias the upper part of the curve is ignored.

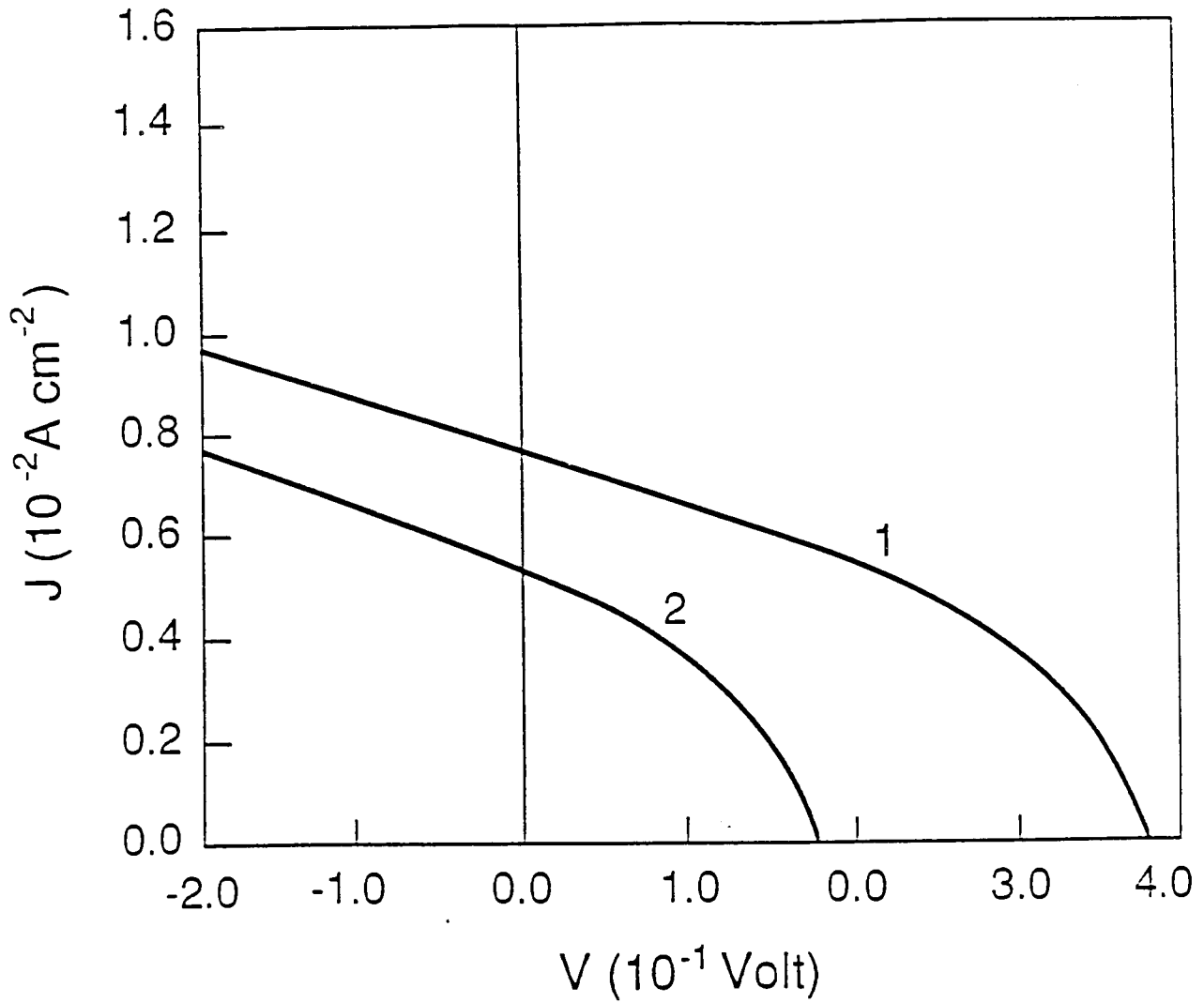


Fig 4-3 The variation of the current density with the voltage from the model for different energies. Illumination is 100 mW/cm^2 .

1. $(E_1 - \mu) = 0.3 \text{ eV}$

2. $(E_1 - \mu) = 0.5 \text{ eV}$

BIBLIOGRAPHY

1. D. L. Pulfrey, "Photovoltaic power generation," Van Nostrand Reinhold Company, New York, 1978.
2. S. M. Sze, "Physics of Semiconductor Devices," John Wiley and Sons Inc., New York, 1984.
3. M. A. Green, F. D. King and J. Shewchun, Solid State Electronics, vol.17, p.551, 1974.
4. M. Capizzi and A. Mittiga, Physica 146 B, p.19, 1987.
5. P. H. Robinson and R. V. D'Aiello, Appl. Phys. Lett. 39 (1), p.63, July 1981.
6. A. J. Tavendale and A. A. Williams, Appl. Phys. Lett. 48 (9), p.590, March 1986.
7. S. J. Pearton, J. W. Corbett and T. S. Shi, Appl. Phys. A 43, p.153, 1987.
8. K. J. Chang and D. J. Chadi, Phys. Rev. Lett., vol.60, no.14, p.1422, 1988.
9. J. Kassobobov, D. Dimitrov and A. Grueva, Solid State Electronics 31, no.1, p.49, 1988.
10. K. Schmalz, R. Krause, H. Richter and K. Tittelbach-Hermrich, Phys. Stat. Sol. (a) 100, K123 (1987).
11. A. Rohatgi, D. L. Meier, P. Rai-Choudhury, S. J. Fonash and R. Singh, J. Appl. Phys. 59 (12), p.4167, June 1986.
12. A. Ourmazd, D. W. Taylor, J. A. Rentschler and F. Bevk, Phys. Rev. Lett., vol.59, no.2, p.213, July 1987.
13. L. L. Kazmerski, A. J. Nelson and R. G. Dhere, J. Vac. Sci. Technol. A 5(4), p.1994, 1987.
14. C. T. Sah, J. Y. C. Sun, and J. J. T. Tzou, Appl. Phys. Lett. 43(2), p.204, July 1983.
15. N. M. Johnson, C. Herring and D. J. Chadi, Phys. Rev. Lett., vol.56, no.7, p.769, Feb. 1986.
16. M. L. W. Thewalt, E. C. Lightowers and J. I. Pankove, Appl. Phys. Lett. 46(7), p.689, April 1985.
17. M. Stutzmann, J. Harsanyi, A. Breitschwerdt and C. P. Herrero, Appl. Phys. Lett. 52(20), p.1667, May 1988.

18. R. J. Van Overstraeten and R. P. Mertens, "Physics, Technology and use of Photovoltaics," Adam Hilger Ltd., England, 1986.
19. C. H. Seager and D. S. Ginley, J. Appl. Phys. 52(2), p.1050, Feb. 1981.
20. C. H. Seager, D. S. Ginley and J. D. Zook, Appl. Phys. Lett. 36(10), p.831, May 1980.
21. L. Ammor and S. Marionuzzi, Solid State Electronics, vol.29, no.1, p.1, 1986.
22. S. Marinuzzi, L. Ammor, M. Sebbar and G. Mathian, 6th E. C. Photovoltaic Solar Energy Conference, Reidel, p.1026, 1985.
23. D. S. Ginley and R. P. Hellmer, 17th IEEE Photovoltaic Specialists Conference, vol.17, p.1213, 1984.
24. L. L. Kazmerski, 6th E. C. Photovoltaic Solar Energy Conference, Reidel, p.84, 1985.
25. J. I. Hanoka, C. H. Seager, D. J. Sharp and J. L. G. Panitz, Appl. Phys. Lett. 42(7), p.618, April 1983.
26. X. C. Mu, S. J. Fonash, B. Y. Yang, L. Vedam, A. Rohatgi and J. Rieger, J. Appl. Phys. 58(11), p.4282, Dec. 1985.
27. C. Dube, J. I. Hanoka and D. B. Sandstrom, Appl. Phys. Lett. 44(4), p.425, Feb. 1984.
28. J. C. Muller, Y. Ababou, A. Barhdadi, E. Courcelle, S. Unamuno, D. Salles and P. Siffert, Solar cells 17, p.201, 1986.
29. V. J. Rao, W. A. Anderson and F. Kai, " Grain Boundary in Semiconductors," Elsevier Science Publishing Company, Inc., p.229, 1982.
30. D. L. Meier, A. Rohatgi, R. B. Campell, P. Alexander, S. J. Fonash and R. Singh, 17th IEEE Photovoltaic Specialists Conference, vol.17, p.427, 1984.
31. L. Sardi, S. Pidatella and G. Figari, Journal de Physique, colloque C1, Supplement au no.10, tome 43, p.125, Oct. 1982.
32. J. P. Hirth and J. Lothe, "Theory of dislocations," J. Wiley and Sons, Inc., 2nd ed., 1982.
33. W. M. R. Divigalpitiya, Ph. D. Thesis, 1988.
34. J. G. Lee, M. Sc. Thesis, 1988.

35. R. H. Glaenzer and A. G. Jordan, Solid State Electronics, vol.12, p.247, 1969.
36. R. H. Glaenzer and A. G. Jordan, Solid State Electronics, vol.12, p.259, 1969.
37. A. L. Fahrenbruch and R. H. Bube, "Fundamentals of Solar Cells," Academic Press, New York, 1983.
38. N. M. Johnson, Phys. Rev. B, vol.31, no.8, p.5525, April 1985.
39. G. Barbottin and A. Vapaille, ed., "Instabilities in Silicon Devices," vol.1, Elsevier Science Pub., B. V., 1986.
40. J. Shewchun, M. A. Green and F. D. King, Solid State Electronics, vol.17, p.563, 1974.
41. J. A. St. Pierre, R. Singh, J. Shewehun and J. J. Loferski, 12th IEEE Photovoltaic Specialist Conference, p.847, 1976.
42. M. A. Green, F. D. King and J. Shewchun, Solid State Electronics, vol.17, p.551, 1974.
43. J. W. Corbett, J. L. Lindstrom, S. J. Pearton and A. J. Tavendale, Solar cells 24, p.127, 1988.
44. J. I. Pankove, R. O. Wance and J. E. Berkeyheiser, Appl. Phys. Lett., vol.45, no.10, p.1100, 1984.
45. F. F. Ho, P. A. Iles and C Cheng, 17th IEEE Photovoltaic Specialist Conference, vol.17, p.591, 1984.
46. J. D. Joannopoulos and G. Lucovsky, editors, " Topics in Applied Physics," vol.56, Springer-Verlag, p.51, 1984.
47. P. Deak, L. C. Snyder and J. W. Corvett, Phys. Rev. B, vol.37, no.12, p.6887, April 1988.
48. C. G. Van de Walle, Y. Bar-Yam, S. T. Pantelides, Phys. Rev. Lett., vol.60, no.26, p.2761, June 1988.
49. P. Gupta, V. L. Colvin and S. M. George, Phys. Rev. B, vol.37, no.14, p.8234, May 1988.
50. B. B. Nielsen, J. U. Andersen and S. J. Pearton, Phys. Rev. Lett., vol.60, no.4, p.321, Jan. 1988.
51. J. I. Pankove, P. J. Zanzucchi, C. W. Magee and G. Lucovsky, Appl. Phys. Lett., vol.46, no.4, p421, Feb. 1985.
52. N. M. Johnson and C. Herring, Phys. Rev. B, vol.38, no.2, p.1581, July 1988.